1965

The fabrication and emission of gallium arsenide lasing diodes

Robert Eugene Cavins
Iowa State University

THE FABRICATION AND EMISSION OF GALLIUM ARSENIDE LASING DIODES

by

Robert Eugene Cavins

A Dissertation Submitted to the
Graduate Faculty in Partial Fulfillment of
The Requirements for the Degree of
DOCTOR OF PHILOSOPHY

Major Subject: Electrical Engineering

Approved:

Signature was redacted for privacy.

In Charge of Major Work

Signature was redacted for privacy.

Head of Major Department

Signature was redacted for privacy.

Dean of Graduate College

Iowa State University
Of Science and Technology
Ames, Iowa

1965

TABLE OF CONTENTS

INTRODUCTION

The concept of an "aser" was first proposed by C. H. Townes in the early 1950's. The word "aser" is an acronym for "amplification by stimulated emission of radiation". In 1954, Townes successfully operated an aser employing ammonia gas. This device was operated at microwave frequencies. Microwave asers have since come to be known as masers. Since 1954 and especially since 1960, a great deal of work has been done on asers including those operating at optical frequencies. These light asers have since come to be known as lasers. In 1960, Maiman (11) successfully operated the first ruby laser. Within a few months the feasibility of gaseous lasers was demonstrated.

In late 1962 Hall et al. (6), Nathan et al. (14) and Quist et al. (18) independently announced the successful operation of a GaAs diode laser. In December of 1962, Holonyak and Bevacqua (8) reported similar laser properties in $Ga(As_{1-x}P_x)$. Since that time, the theory and techniques involved with P-N junction lasers have been developing at a rapid pace. This thesis will consider both the area of fabrication and the theory of operation of junction lasers.

This thesis is divided into two areas: 1. Fabrication

of GaAs P-N junction diodes and 2. Emission characteristics and theory of GaAs diodes.

Although GaAs lasers are presently being produced in many laboratories, the fabrication techniques are still being developed. This thesis will discuss techniques which require a minimum of equipment, no controlled atmospheres, and readily available materials. Most authors describe their diodes as being made with "standard semiconductor techniques". Hopefully, this thesis will illuminate these techniques.

The second area concerning the emission spectra will cover the theory of expected emission and the actual measured data. Although much theory has been developed concerning the diode laser, no completely satisfactory explanation of the emission mode structure has been offered. This and other parts of the theory will be discussed.

BACKGROUND

Since the only difference between a maser and a laser is the wavelength of the coherent emission, any comments made in this thesis will generally apply to both masers and lasers. The wavelength for a maser falls in the microwave range while a laser has wavelengths in the optical range which includes the visible wavelength spectrum. The experimental work described in this thesis was performed on GaAs which has an emission output around 8400 A^{o}. This wavelength is located in the near-infrared region of the electromagnetic spectrum and as such is very close to the visible range. Since it is so near the visible spectrum, the GaAs emitting devices are classed as lasers.

The basic ideas involved in a laser or maser are neither involved nor complex. Quantum mechanics tells us that a bound particle can have only certain discrete energies. Furthermore, we know that particles have a lowest preferred energy state which is usually called the ground state. Higher energy states are referred to as the excited states. If a particle undergoes a transition from an energy state E_1 to a state E_2 with a change of energy ΔE then the particle either absorbs or releases energy ΔE depending on whether E_1

or E_2 is the more excited state. If a particle is in an excited state, it has a statistical lifetime before it will spontaneously release energy and fall down to some lower energy state. This energy release may appear as either a phonon or photon or a combination of both. Of course, the release of energy in the form of a photon is necessary for a laser. Although there seems to be no theoretical reasons why a transition involving a phonon and photon cannot be used, Dumke (4) gives some practical reasons why such a transition does not lend itself for laser use.

In addition to spontaneous emission of energy, in some cases an excited particle may be stimulated by a passing photon to release energy and fall back to a lower energy level. It has been found that, if the energy difference between two energy levels is E, a photon of energy E can stimulate the excited particle to release a photon which is identical to the impinging photon. This process involves a lossless interaction and thus one photon and one excited particle will result in two photons and one unexcited particle. Since the second photon is identical in temporal and spatial variations with the first one, the radiation is said to be coherent. Thus, we now have a possibility of producing a laser if these

properties can be incorporated into a device which uses this coherent radiation as an output.

The first prerequisite for a lasing system must be a system with discrete allowed energy levels such as found in GaAs. The second prerequisite must be some means of populating excited states. A third prerequisite must be a high stimulated emission probability. Einstein's A and B coefficients show that the stimulated emission probability is directly proportional to the spontaneous emission probability. A high spontaneous emission probability implies the radiative lifetime in the excited state must be short. Thus a short radiative lifetime is also necessary.

At this time it should be noted that the primary function of a laser depends on obtaining the stimulated emission external to the lasing system. However, if one should extract too much of the available radiation, the internal regenerative processes would be broken and the output would be extinguished momentarily. Therefore the system must allow the extraction of a certain fraction of the available radiation with the remaining internal radiation being used to sustain the stimulation processes. In this way the process can be maintained.

Figure 1 shows a structure which has been used successfully as a lasing structure. Excited particles are injected into the active region from regions I and II. The radiation is stimulated and a pyramiding action occurs as the radiation passes through the crystal. When the radiation reaches the end, a reflective coating allows some radiation to escape while the remaining radiation is reflected back into the crystal to maintain the stimulation process. Note that regions I and II act to guide the radiation between the two ends. In a gaseous laser, the reflecting ends are obtained by placing reflecting mirrors in the path of the radiation. Typical mirrors have a reflectivity of about 99 per cent. The excited states are obtained by maintaining a gaseous discharge at an appropriate level.

In the lasers to be discussed in this thesis, this structure is actually a solid block of GaAs or perhaps some other suitable semiconductor. Regions I and II of Figure 1 are either N- or P-type doped material and the active region is near the depletion region of the P-N junction.

GaAs seems to be a good material for solid state lasers for several reasons. The band gap is around 1.5 eV which corresponds to a wavelength of about 8400 A^{o} and is thus in

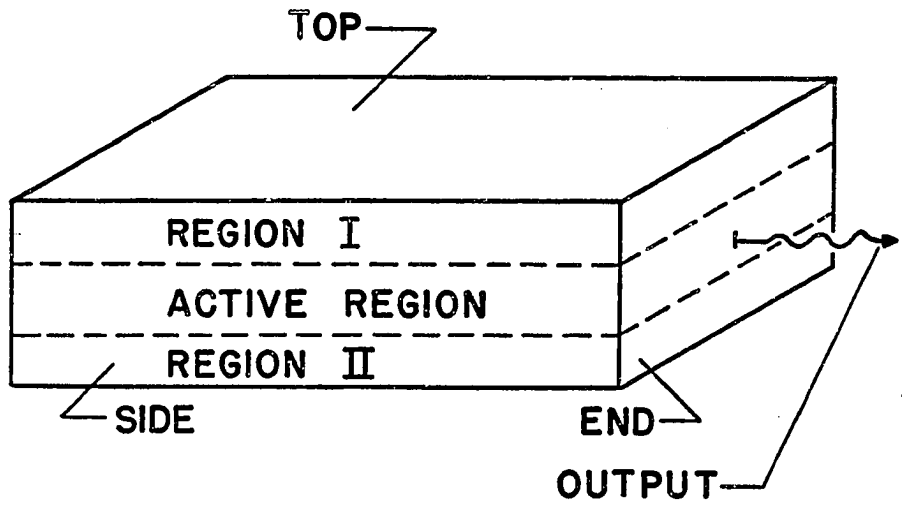

Figure 1. A simple structure capable of sustaining laser action

a range of ready measurement with existing optical instruments. Its index of refraction, $\bar{n}$, is about 3.30. The reflection coefficient for a wave traveling in a medium with index of refraction, $\bar{n}$, with normal incidence on an air interface, is given by the equation

$$R = [(\bar{n} - 1)/(\bar{n} + 1)]^2 \qquad (1)$$

With $\bar{n}$ equal to 3.30, R is about 0.32. This means that about two-thirds of the impinging radiation will be the output while one-third will be returned into the active region to sustain the stimulation process. This one-third seems to be adequate and thus the ends of a GaAs crystal will need no reflective coatings if they are prepared very flat and perpendicular to the active region. It has been found that the GaAs crystal has the zincblende crystal structure and that it may be readily cleaved to give optically flat surfaces which serve very well as the reflecting ends. The excited particles for this laser are supplied by passing current through a forward biased diode. Figure 2 shows how the electrical carriers are assumed to appear before and after forward biasing. The forward current in effect places electrons in the conduction band of the P-side and holes in

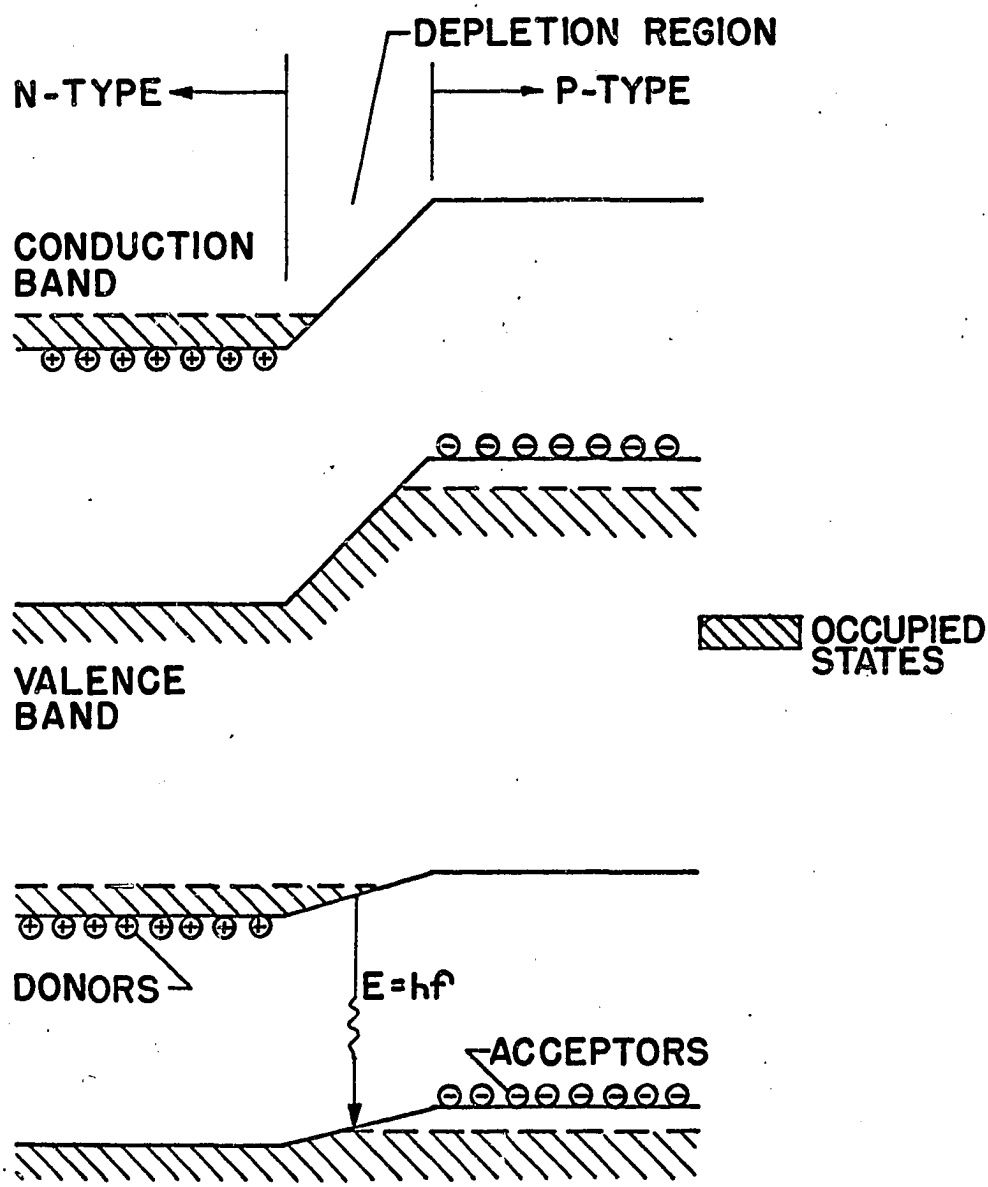

Figure 2. Diagrams of a P-N junction under zero bias (top figure) and under a bias of E_g/e volts (lower figure)

the valence band of the N-side. In the active junction region these carriers combine and the energy released is approximately the band gap energy of 1.5 eV. This energy is released in the form of a photon. A detailed discussion of electron-hole theory can be found in Dekker (2). Information on P-N junctions can be found in Phillips (16).

FABRICATION

The fabrication of any device depends on the desired final product. The final product is a GaAs P-N junction diode. This diode crystal is a rectangular parallelepiped as shown in Figure 1. The diode thus has two sides and two ends. The top and bottom P-type and N-type layers are parallel to the junction. The diode ends must be flat and perpendicular to the junction in order to furnish reflected radiation back into the junction. The sides can be either flat or rough and need not be perpendicular to the junction. If the laser beam is desired from only one direction, the sides should not be able to reflect enough light to allow lasing in any modes involving reflection from the side surfaces. This entire preparation of the crystal can be done most easily by diffusing the junction into a crystal wafer oriented in the [100] direction. Dill (3) explains that the ends can be cleaved along the $\{110\}$ planes which give both optically flat faces and faces which are perpendicular to the junction. The sides can be cleaved also. For directional diodes, the sides can be sawed to yield a rough surface to depress all internal reflection from these sides.

The discussion of fabrication will be divided into

steps. These are: (1) crystal preparation, (2) junction diffusing, (3) polishing, (4) plating the contacts, (5) cleaving, (6) sawing, and (7) mounting the crystal.

Crystal Preparation

The crystals for GaAs diodes must be single crystals with the proper doping levels. Most workers recommend starting with an N-type crystal with the donor agent usually being tellurium. Burns and Nathan (1) give $3x10^{17}$ to $6x10^{18}$ carriers per cm^3 as the limits of N-type impurity concentration for good low-threshold GaAs lasers. An impurity concentration of 10^{18} seems to be a good level for diode fabrication. Low doping levels result in very high current requirements while high doping levels produce radiation approaching the absorbtion edge of GaAs. The crystals used in this work were acquired from the IBM Corporation. Table 1 shows the parameters for the two crystals used in the work discussed in this thesis.

The orientation of crystal number 1 was known while that of crystal number 2 was not. Laue X-ray back-reflection patterns were used to locate the $\{001\}$ plane. The crystals were then cut into wafers with the face of the wafers being

Table 1. GaAs crystal data

Crystal number	Basic material	Donor	Net donor concentration per cm^3	μ	ρ ohm-cm
1	N-type GaAs	Tellurium	6.8×10^{18}	--	0.00033
2	N-type GaAs	Tellurium	1.89×10^{18}	2820	0.00117

the {001} plane. This orientation was chosen because the {110} faces are perpendicular to the {001} face. See Dekker (2) for a discussion on crystallographic structures.

The wafers were cut with a spark cutter using a continuous copper wire. However other tools such as a diamond saw can be used. After cutting, the surfaces were lapped to assure smoothness. The cut wafers are approximately 12 to 15 mils thick. It is extremely important that the face of this wafer be perpendicular to the {110} cleavage planes. The wafer was then cleaved and, using the equipment shown in Figure 3, the planes were checked. This method was used by Proebsting (17). After alignment the wafer was polished to a flat surface using successive steps of abrasive compounds in

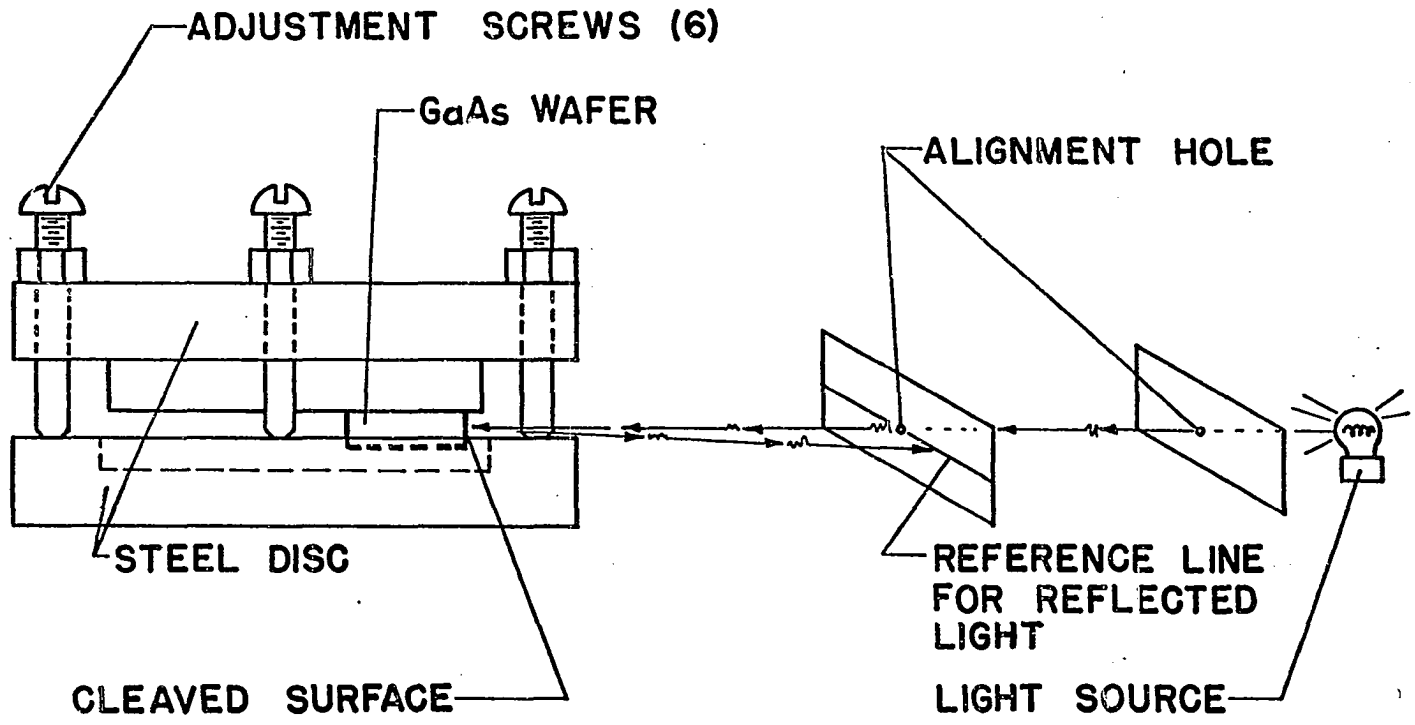

Figure 3. Sketch showing the method used to orient the GaAs wafer face perpendicular to the 110 crystal planes

the following order: (1) 400 mesh Carborundum, (2) 600 mesh Carborundum, (3) 1200 mesh Carborundum, (4) 1 micron alumina, and (5) 0.3 micron alumina. These abrasives are commercially available and can be purchased from most metal finishing suppliers.

If all of these steps have been done well, the wafer ends up with both sides polished to a smooth finish. The faces are parallel and are located on {001} crystal planes. The wafer was now about 7 to 12 mils thick.

Junction Diffusing

Since the starting material is N-type, the P-type layer must be formed by diffusing an acceptor atom into the N-type material. For GaAs, this diffusant is usually zinc. Hilsum and Rose-Innes (7) state that, for temperatures below 800° C, spatial distribution for zinc diffusing into GaAs is a complimentary error function of the surface concentration of the diffusant. Above 800° C, the distribution is not a simple one. Figure 4 shows the distribution as a function of the zinc concentration.

In order to avoid contamination of the surface, the diffusion of zinc atoms into the GaAs crystal was done under vacuum. This is illustrated in Figure 5. The diffusant is

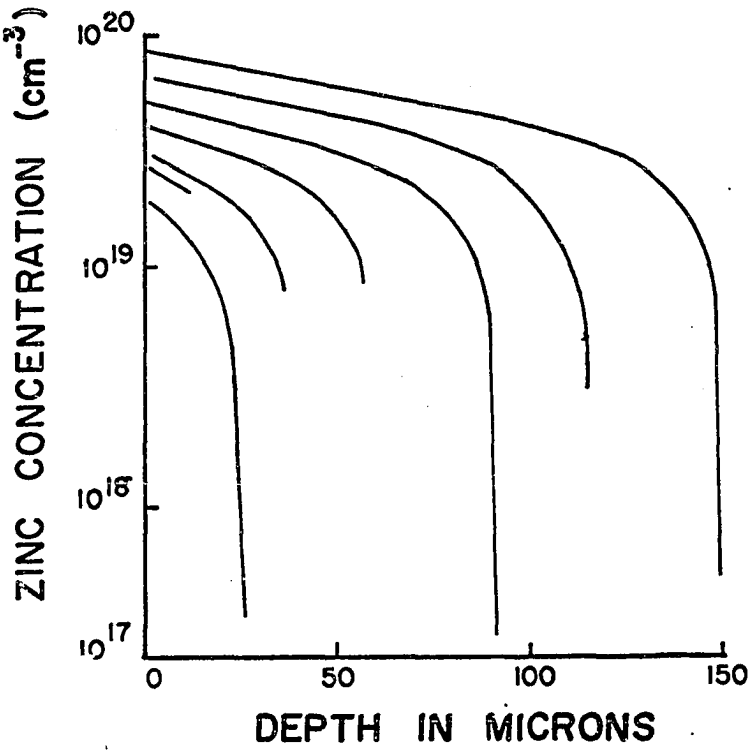

Figure 4. Diffusion of zinc into GaAs after 10^4 sec at 1000° C

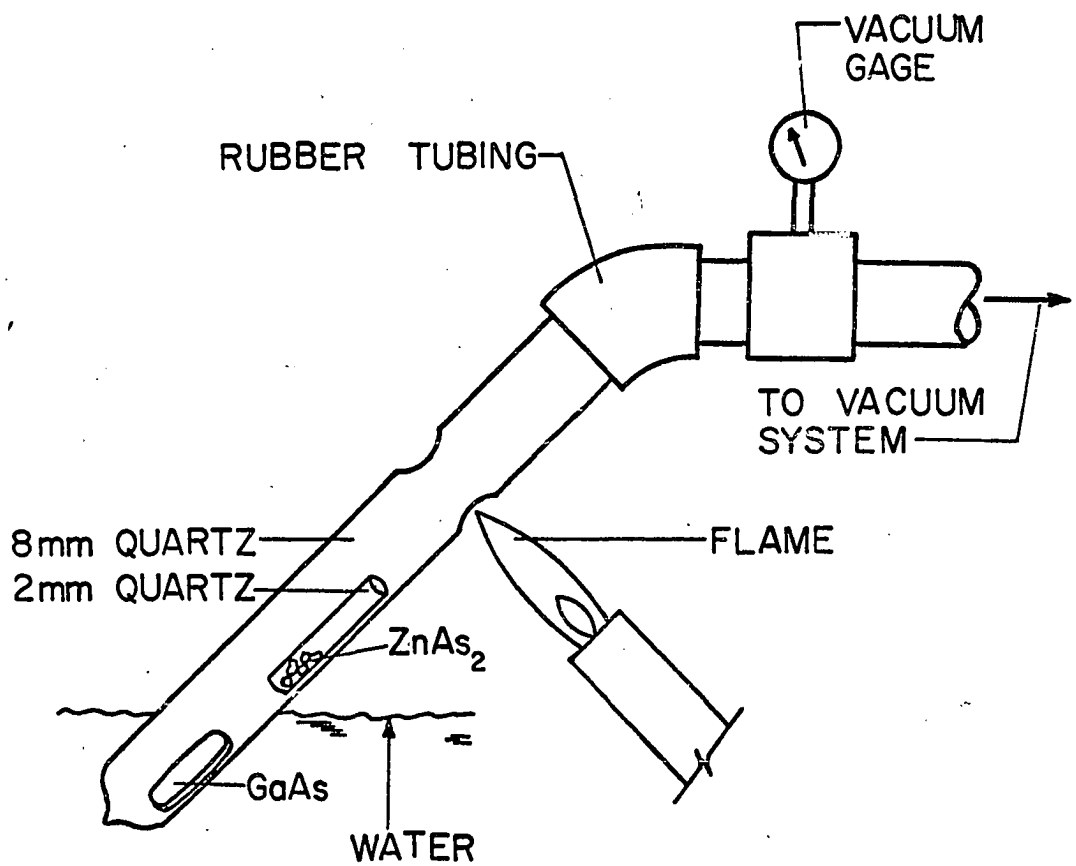

Figure 5. Method of encapsulating the GaAs wafer prior to diffusion

$ZnAs_2$ in a crystalline form. The amount of diffusant was approximately 5 mg and the volume of the encapsulating vessel was about 2 cubic centimeters. Most writers recommend 3-16 hours at 850 C. Figure 6 shows a typical temperature cycle used for diffusing the zinc. This cycle produced P-type layers about 3 mils in depth. It is possible to see the P-N junction if the wafer is cleaved and the cleaved face is etched with a basic solution. Proebsting (17) suggests the following solution:

10:1:1 H_2O:HF:H_2O_2

Thirty seconds should be adequate to etch the junction. Water is used to rinse the etchant from the crystal. The crystal should then be dried and the junction observed under a microscope. This etching solution was used and proved satisfactory. Several authors suggest using KOH for the etchant. The furnace used for this work has a rectangular heating chamber which is approximately 4 inches on a side. Care should be taken to ensure uniform temperatures spatially over the wafer surfaces. The vacuum pressure used was about 1 micron or 10^{-3}mm Hg, which can be accomplished with a good roughing pump.

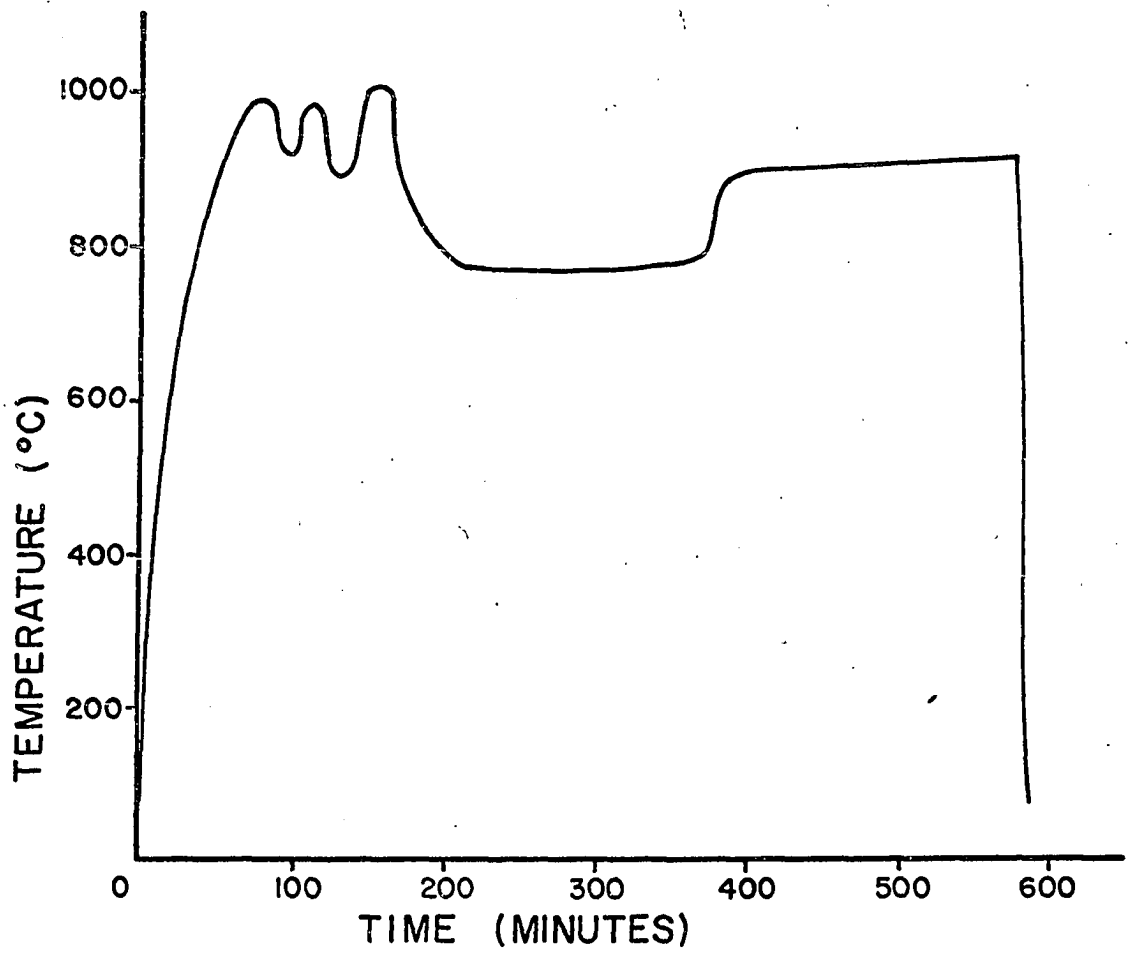

Figure 6. Graph of the diffusion temperature versus time for the diffusion of zinc into GaAs

Plating the Contacts

At this point the diffused wafer resembles a transistor more than a diode. The structure is typically a P-N-P wafer with the P-type layers on both sides about 3 mils thick. To obtain diodes, one of the P-type sides must be removed. In addition, there will be non-stoichometric deposits of zinc, arsenic, and gallium on the other side. Both sides are hand polished with 1200 mesh Carborundum abrasive. About 5 mils are removed from one side and 1 mil is removed from the other. This yields a wafer which is 4 mils thick with the P-N junction located approximately half-way between the faces.

It has been found that conventional solders do not readily wet GaAs. Therefore, to make contacts to the diode faces, one must carefully prepare the surface. The method used closely parallels the method by Proebsting (17).

The wafer is electroless plated with nickel and this nickel is thermally treated on the crystal. This nickel surface gives negligible contact resistance and is readily wetted by commercial solders.

The wafer is first plated for 15 seconds, at room temperature, with gold in the following solution:

4 parts	$AuCl$	1 gram
	H_2O	500 ml
1 part	HF (48%)	

The wafer will appear to have a yellowish color. The wafer is then plated for 2 minutes in a nickel solution at 98 C. The nickel solution is:

$NiCl_2 \cdot 6H_2O$	3	grams
$NaH_2PO_2 \cdot H_2O$	1	gram
$(NH_4)_2HC_6H_5O_7$	6.5	grams
NH_4Cl	5	grams
H_2O	100	ml

Add NH_4OH drop by drop until solution turns from green to blue. Add NH_4OH as necessary to maintain blue color.

The wafer is a nickel gray color after this plating. It should be noted that the temperature must be near 100^{o} C and that this temperature can be maintained by placing a small beaker of the plating solution in a boiling water bath. Bubbles will come from the wafer when the plating starts. The two minutes should start when the plating or bubbling starts. If the plating does not start, the trouble

is usually caused by a low temperature of the plating bath.

The wafer then receives another 15 second plating of gold. This yellowish gold color will be used as an indicator in the thermal treatment of the nickel. The wafer is then placed on a 7 mils thick glass slide which is on a hot plate. An estimate of the temperature is 600° F. At this temperature the gold is dissolved into the nickel and the gold color is replaced by the gray color as the nickel becomes strongly bound to the wafer. This surface is now prepared for easy soldering.

It should be noted that the etching solution described on page 18 can not be used to observe the junction after plating. The solution causes nickel to deposit on the cleaved surface and no junction is observable. Also, the heating of the nickel plate can be done in a hydrogen atmosphere or vacuum. Either of these two atmospheres is preferred to the air.

In addition to this method, permalloy contacts were attempted using vacuum deposition techniques. The permalloy (or other vacuum deposited metal film) can be applied at low temperatures. This would eliminate unnecessary heating of the wafer. Some solder tests were made and it was found that

it was easier to solder to permalloy. The vacuum deposition also eliminates the use of plating baths and the cleanliness problems which accompany these solutions. The permalloy did not adhere to the wafer and this method was abandoned. It was felt that if the wafer were properly heated, good adhesion could be produced and these contacts would be superior to the tin plating.

Cleaving

After plating the wafer is about 4 mils thick with all surfaces nickel plated. The crystal must now be cleaved along $\{110\}$ planes. The separation of two adjacent cleavage planes will be the length of the final diode. These cleavage planes should be parallel to the plane used to align the crystal as described in Figure 3. If the [001] axis is perpendicular to the surface of the wafer, the wafer can be cleaved along a $\{110\}$ plane which is perpendicular to the $\{1\bar{1}0\}$ plane. However there is no assurance of this condition. Therefore the cleavage should be along the $\{110\}$ plane.

To cleave the wafer, a sharp edge is placed against the wafer and pressure is applied to the wafer in such a way as to crack the wafer along the $\{110\}$ planes. This is most

easily done by using a sharp dissecting knife with a rounded blade. This blade can be rolled onto the wafer parallel to the $\{110\}$ planes. A soft base should be supplied for the wafer. It was found that a piece of plexiglas with a thin piece of manila paper pasted to it was about right. The entire operation should be performed under water or some suitable liquid. This eliminates motion of the crystal after cleaving. The cleaving must be observed under a microscope. However the best measure of cleavage is the sound and consequently, quiet environments are necessary. The sound of cleavage is quite discernible.

The ends of the diode cavities were formed by cleaving the crystal. Although this seems to be the easiest method, it does require the proper orientation of the crystal. Some workers circumvent the problems of orientation by polishing the ends flat and parallel. Again these techniques work well but are extremely difficult to use without specialized equipment.

Sawing

The crystal by now is a long, thin rectangular bar with the two sides being cleavage planes and the top and bottom

nickel plated. One must now cut the crystal on the $\{1\bar{1}0\}$ planes. This rough surface will force all lasing modes to be reflected off the cleaved sides only. For ease in cutting the crystal bars were mounted completely in plexiglas and the cutting done by a wire abrasive saw. The saw used in this construction was a Bay City Technology Group Model 716 saw with 600 mesh Carborundum abrasive suspended in a solution of glycerol and water. The finished crystals are small six sided parallelepipeds with two ends cleaved, two sides sawed, and the top and bottom nickel plated.

It is also possible to cleave the sides as well as the ends. If directional diodes are desired, these sides may then be roughened by rubbing a wire through an abrasive slurry and across the side surfaces. This method was attempted with inconclusive results.

Mounting

The diode crystal should be mounted on a permanent base. Transistor TO-5 headers were used as a standard base. Figure 7 shows a sketch of a finished diode mounted on its TO-5 header. The mounting requires soldered contacts at the top and bottom of the crystal. The TO-5 header was held in a vise and all work is done under a microscope. A 30X power micro-

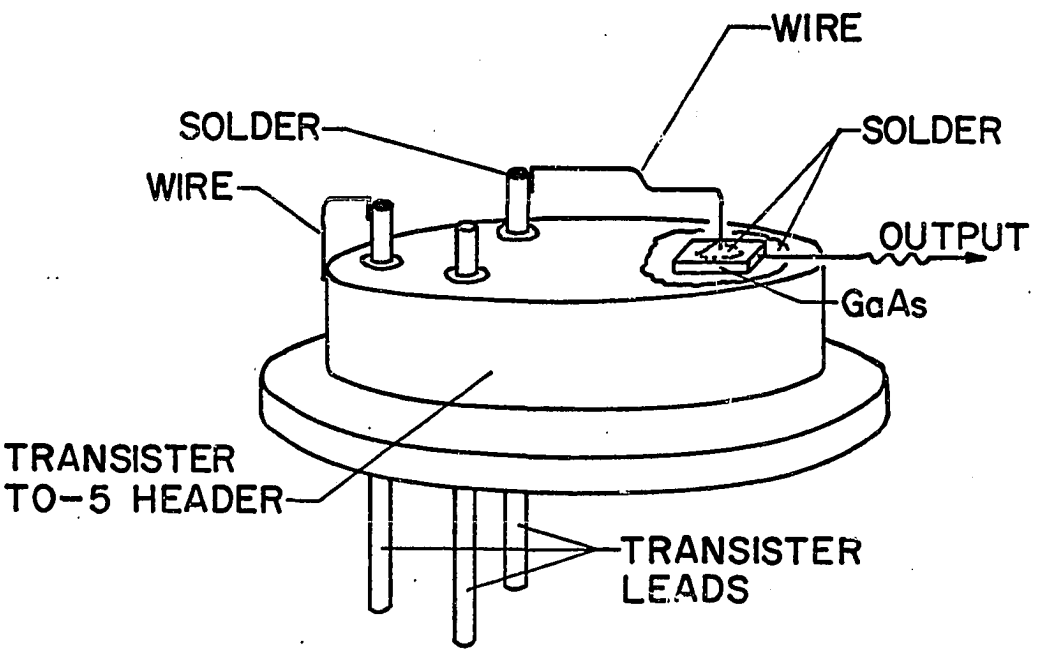

Figure 7. Sketch of typical diode mounting

scope was found to work satisfactorily. The solder used was standard 60-40 lead-tin radio solder. The flux used was NoKoRode brand rosin flux.

A small spot of solder flux was applied to the spot chosen for the diode location. A small piece of solder was then cut from a flat sheet of solder and this small piece was placed on the flux. The header was then heated by applying a soldering gun or soldering pencil to the body of the header. The conducted heat melted the solder which wetted the header. Some additional flux was placed on the still warm solder and then wiped away. This left a clean surface on which to place the diode crystal. The flux was found to be the best solvent for removing any residue from the surface of the solder after heating. Clean flux was then placed on the solder spot and the diode crystal was placed on the solder flux. The crystal was best transported by using a knife point wetted with flux. The crystal readily adhered to the flux and could easily be deposited on the solder spot. This operation was difficult at first but was readily mastered with a little practice.

Again, conduction heat was used to melt the solder and thereby solder the crystal to the header. A small amount of flux was next applied to the top of the crystal and a very

small piece of solder (2 mils square) was placed on it. Heating the header caused the solder to melt and wet the top surface.

The last part of fabrication involved placing the top wire-contact in place. The 2 mil diameter copper wire that was used was pre-tinned and soldered to the transistor lead. This wire was bent slightly and oriented so as to be tight against the solder on top of the crystal. During one last heating of the header, the wire was bonded to the crystal and the diode completed.

This technique of fabrication was found to work satisfactorily. Some authors mention making the electrical contacts with silver paste instead of solder. Although silver paste does make excellent electrical contact to GaAs, it is very difficult to handle for small diodes and this method was abandoned. Marinace (12) states that good electrical contacts can be made with pressure contacts. No attempt at this method was tried.

The solder used was in a sheet form and was cut into the proper size pieces with a dissecting knife. The solder sheet can be easily prepared from regular wire solder by melting

the solder and allowing the drops to fall about 4 feet onto a flat clean piece of glass. The 2 mil diameter wire can be found in small sizes of standard stranded conductors.

VOLT-AMPERE CHARACTERISTICS

Although the main purpose of the lasing diode is the emission of coherent radiation, the diode is basically an electrical device. After the diodes were fabricated, the volt-ampere characteristics of each diode were checked with the circuit shown in Figure 8. It is possible for the diodes to be shorted or open circuited. Such troubles are readily apparent. If the crystal preparation and diode fabrication have been properly carried out, the volt-ampere characteristics should be as shown in Figure 9. Characteristics of actual diodes prepared in this project are shown in Figures 9 and 10. Figure 9 shows characteristics for both a good and a poor diode. The double bend in the poor diode's characteristics is probably caused by surface effects due mainly to dirty surfaces. Figure 10 shows the characteristics of a typical diode. Notice that it is not idealized and in fact, some surface effects are present. It should be pointed out, however, that the diode will be operated on the vertical part of the V-I curve. Therefore the knee in these characteristics will appear as a leakage current only.

If diodes are prepared with clean techniques, they will appear as in Figure 9. In fact the good diode character-

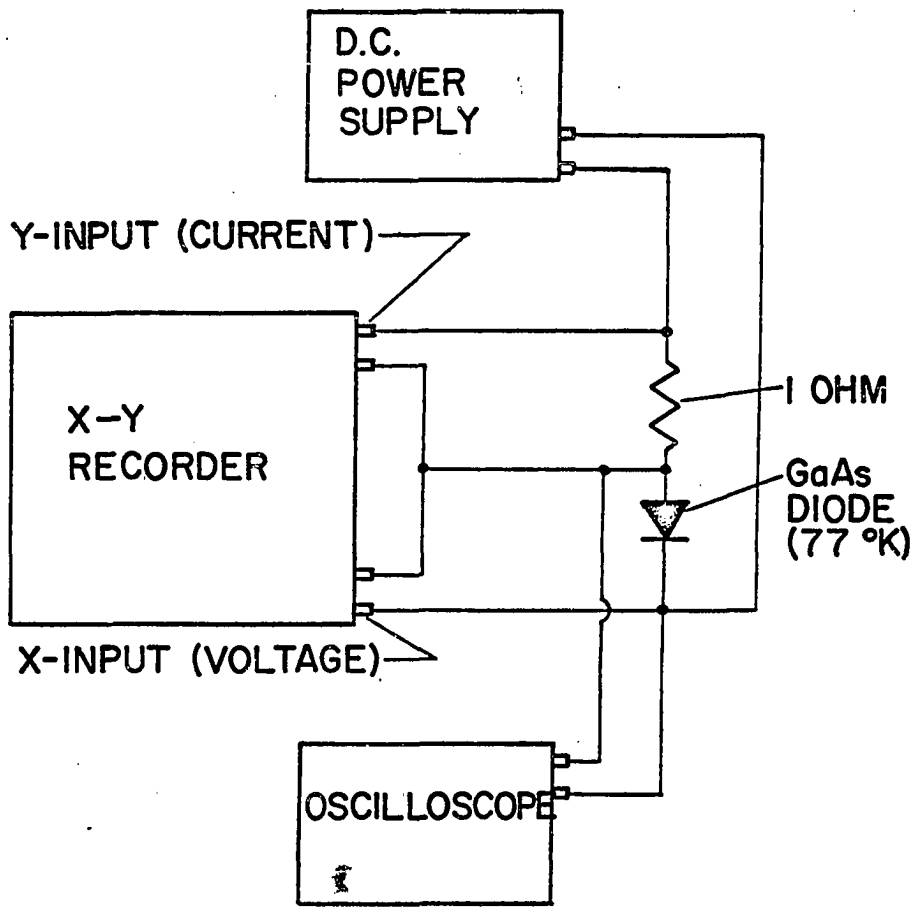

Figure 8. Test arrangement for measuring the volt-ampere characteristics of GaAs diodes

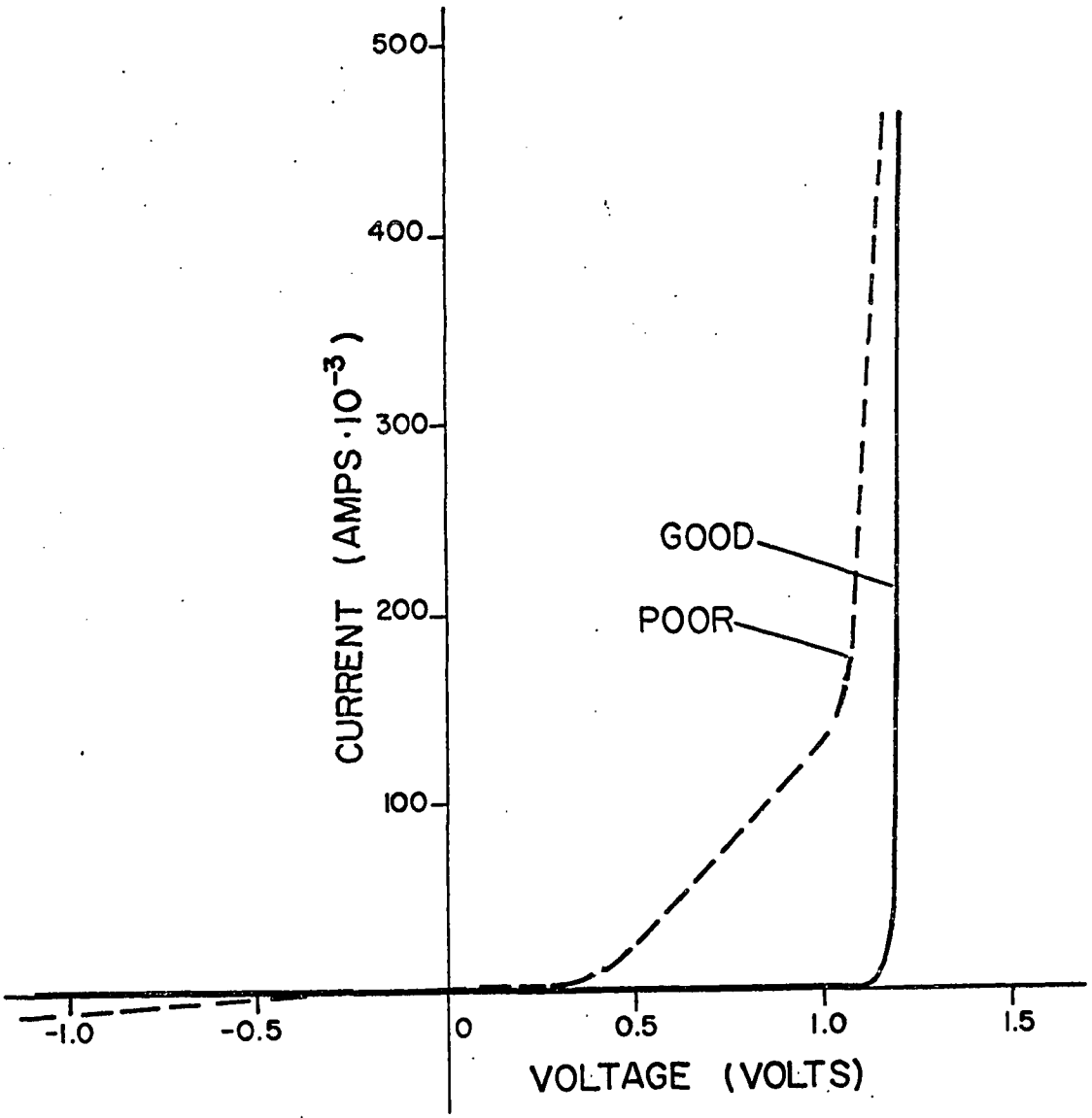

Figure 9. Diode V-I characteristics for good and poor diodes

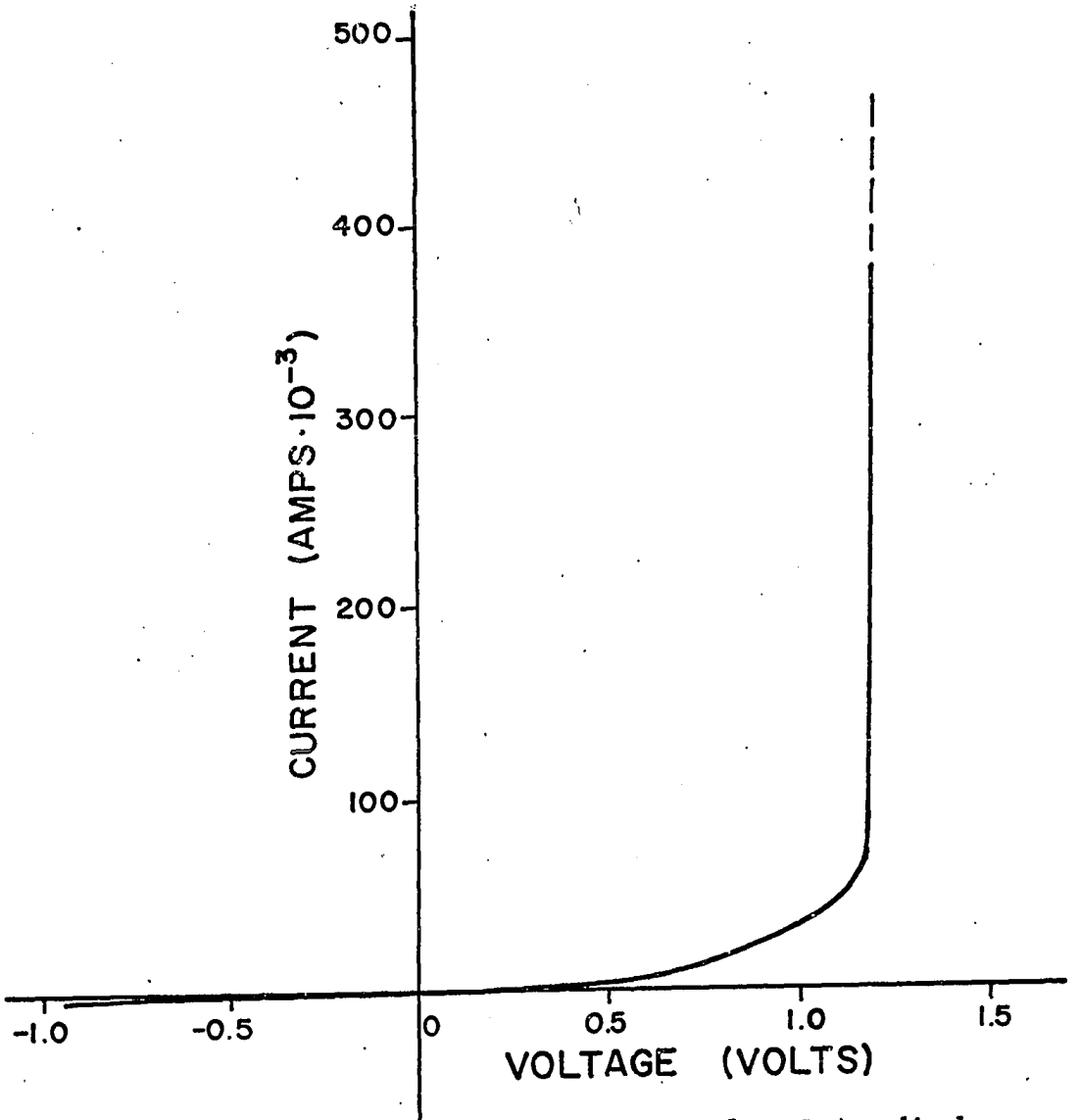

Figure 10. Typical V-I characteristics of a GaAs diode (characteristics shown were taken from diode number 100)

istics shown in Figure 9 were taken from a diode furnished by the Texas Instrument Company. It seems reasonable that due to fragileness, a small crystal could not be cleaned as well as a large crystal. This was found to be true. Diodes having the larger crystals usually exhibited the sharper knees in their V-I characteristics. The same is true with respect to the reverse leakage currents.

EXPECTED EMISSION

Material Properties

If one desires to study the emission of a material such as GaAs, perhaps the first subject should be the energy versus the wave-number, k, diagrams. Figure 11 shows the assumed energy diagram for GaAs. The first important fact concerning Figure 11 is to note that GaAs is a direct transition semiconductor (i.e. the minimum of the conduction band and maximum of the valence band occur at the same value of k). If electron populations are inverted into the conduction band with holes located in the valence band, the electrons can combine with the holes and a photon will be emitted. From Figure 11 this photon is described by

$$hf \geq E_g \tag{2}$$

where h is Planck's constant and f is the frequency of the radiation.

Since most data is expressed in wavelengths, the familiar equation

$$\lambda f = c \tag{3}$$

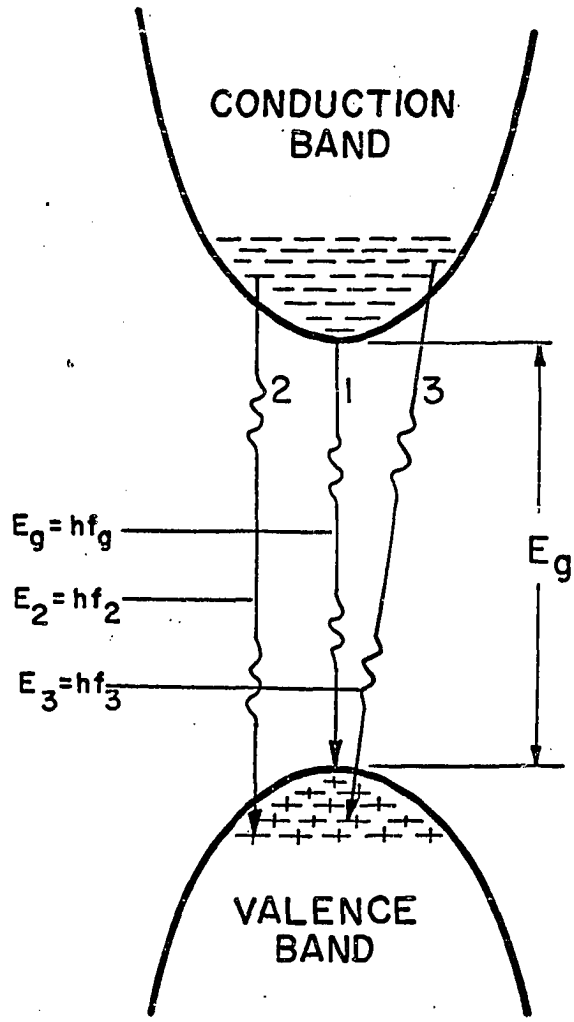

Figure 11. Possible radiation wavelengths from interband transitions

should be used to convert f to λ where f is the frequency of the photon, λ is its wavelength and c is the velocity of light. Combining Equations 2 and 3 gives

$$\lambda \leq hc/E_g \qquad (4)$$

Direct transitions can occur as in transition number 1 of Figure 11. This transition corresponds to the photon of energy E_g. Transition number 2 shows a direct transition of energy greater than E_g and equal to E_2. Transition number 3 involves a transition of energy E_3 from a conduction state to a valence state having a different momentum (wave-number k). This transition usually involves a phonon in order to conserve momentum although with the high impurity concentrations found in lasers, momentum can be conserved by the impurities. In addition to the transitions between bands, electron-hole pairs called excitons may be formed.

This exciton has a binding energy similar to the case of the hydrogen atom. When the electron-hole pair combine, this binding energy is lost to the phonon and results in heating the lattice. Dekker (2) points out that it is possible to estimate the binding energy of an exciton by using the theory of the Bohr atom immersed in a medium with a dielectric

constant the same as that of GaAs. This energy is given by the expression

$$\epsilon_x = - \frac{\mu e^4}{8h^2\kappa^2} \tag{5}$$

where μ is the reduced mass.

$$\mu = \frac{m_e + m_h}{m_e m_h} \tag{6}$$

In Equations 5 and 6, e is the electron charge, κ is the dielectric constant, and m_e and m_h are the electron and hole effective masses respectively.

Equation 5 represents the binding energy of an exciton in an orbit corresponding to the ground state Bohr radius. If the exciton is allowed to have excited states, the binding energies of these excited states are given by the expression

$$\epsilon_{xn} = - \frac{\mu e^4}{8h^2 n^2 \kappa^2} \tag{7}$$

where n = 2, 3, 4, ... Equations 5 and 7 give the binding energies possible for the excitons. If we assume that most transitions will be from the conduction band edge to the valence band edge, the exciton emission energy is given by

$$E_x = E - \epsilon_x = E - \frac{\epsilon_x}{n^2} \tag{8}$$

for n = 1, 2, 3, ...

If we refer back to Figures 2 and 11, it seems possible that in addition to transitions between bands, transitions involving impurity levels may also be involved. These transitions would be from the conduction band to the acceptor levels, and from the donor levels to both the acceptor levels and the valence band. The GaAs normally used for lasers is doped to about 10^{18} impurity atoms per cubic centimeter. At these impurity concentrations Hilsum and Rose-Innes (7) point out that the donor levels are completely merged into the conduction band. Hilsum and Rose-Innes also state that zinc atom acceptor sites occupy levels about 0.08 eV above the valence band. Burns and Nathan (1) have shown that the laser transitions do in fact involve the acceptor levels. Their results indicate the transition of primary importance is from the conduction band to the acceptor levels.

With the preceding ideas in mind it is illuminating to look at absorption spectra for GaAs. This information should give some numerical values to the transitions already mentioned. Sturge (19) clearly shows that both the exciton and band edge adsorption spectra do occur. In addition some absorption is found at longer wavelengths. These are believed

to arise from impurity ionization as well as some deep impurity traps. These however should not appear in the emission spectra. In addition, Sturge gives the binding energy of the exciton as 0.004 eV. Although Sturge's work was done on GaAs having low impurity concentrations, his work does establish the existence of the band-edge and exciton lines. It should be pointed out that while excitons may exist in GaAs, excitons do not generally contribute to laser radiation. GaAs laser radiation depends almost entirely on impurities. A good explanation of optical properties can be found in Moss (13).

One last area to yield useful information on possible emission spectra is low temperature fluorescence experiments. Burns and Nathan (1) give the results of such experiments. These experiments and their results corroborate the previous discussions.

According to Equation 4, wavelengths less than the wavelength corresponding to the band edges are all possible. In reality there are limits on the energy of the emitted radiation. In practice, transitions involving states near the band edges are the most numerous provided these states are filled. With the high donor concentrations, the conduction

states near the band edges can be assumed to be filled. The energy gap between the valence band and the acceptor levels is about 0.08 eV according to Hilsum and Rose-Innes (7). This small gap allows the electrons in the valence band to be elevated to this acceptor level and thus it is reasonable to assume an abundance of holes at the edge of the valence band. The probability of finding electrons at high energies in the conduction band or holes deep in the valence band is small. The net result of these discussions is to limit the emitted radiation to wavelengths corresponding very close to the band-edge emission.

Geometric Properties

If there were no limitations on the emission because of geometry, the output should appear as previously discussed in this section. However, the geometry of the GaAs laser does in fact introduce geometrical considerations. If we start at one end of the crystal, we see that some of the coherent radiation is transmitted while some is reflected toward the other end of the crystal. If coherence in the output is to be maintained, this reflected radiation must travel the length of the crystal and back and be in phase

with the original emission. This can be expressed as

$$m(\lambda/\bar{n}) = 2L \tag{8}$$

where L is the length of the crystal, λ is the free space wavelength of the radiation and $\bar{n}$ is the index of refraction. The mode number m is usually large and must be a positive integer. This is the first restriction derived from the geometry of the diode. Burns and Nathan (1) explain that if Equation 8 is differentiated with respect to λ, one obtains

$$L \frac{d\lambda}{\lambda^2} = \frac{1}{2\bar{n}\left[1 - \frac{\lambda}{\bar{n}} \frac{d\bar{n}}{d\lambda}\right]} \tag{9}$$

To derive Equation 9 it must be recognized that m, λ, and $\bar{n}$ are all functions of λ. In addition, m is assumed large and dm is -1. Burns and Nathan (1) point out that $d\bar{n}/d\lambda$ is very important in this equation and that in the region of emission $d\bar{n}/d\lambda$ is widely varying and difficult to measure. However, certain measurements and approximations can be used to make Equation 9 agree with theory.

The principal discussion in this section will be centered around small crystal dimensions where m is in the order of a few hundred to a few thousand.

If a crystal is emitting a wavelength λ_1, we can rewrite

Equation 8 as

$$\lambda_1 = \frac{2L\bar{n}}{m} \tag{10}$$

where L is the length of the crystal, $\bar{n}$ is the index of refraction and m is a positive integer corresponding to the mode number of λ_1. If more energetic photons can be emitted, the next wavelength to satisfy Equation 8 can be called λ_2 and is given as

$$\lambda_2 = \frac{2L\bar{n}}{m+1} \tag{11}$$

The difference between these wavelengths is given as

$$\lambda_1 - \lambda_2 = \Delta\lambda = \frac{2L\bar{n}}{m(m+1)} \tag{12}$$

In Equation 12, if we assume m + 1 is approximately equal to m and if we substitute for m, we obtain

$$\Delta\lambda = \frac{\lambda}{m} = \frac{\lambda^2}{2L\bar{n}} \tag{13}$$

Figure 12 shows a plot of $\Delta\lambda$ in A^o versus the length of the crystal. This is based on λ equal to 8400 A^o.

The crystal length, L, affects the emission by allowing only certain wavelengths to reinforce themselves. If we assume the band-gap radiation is 8400 A^o, and if we take the

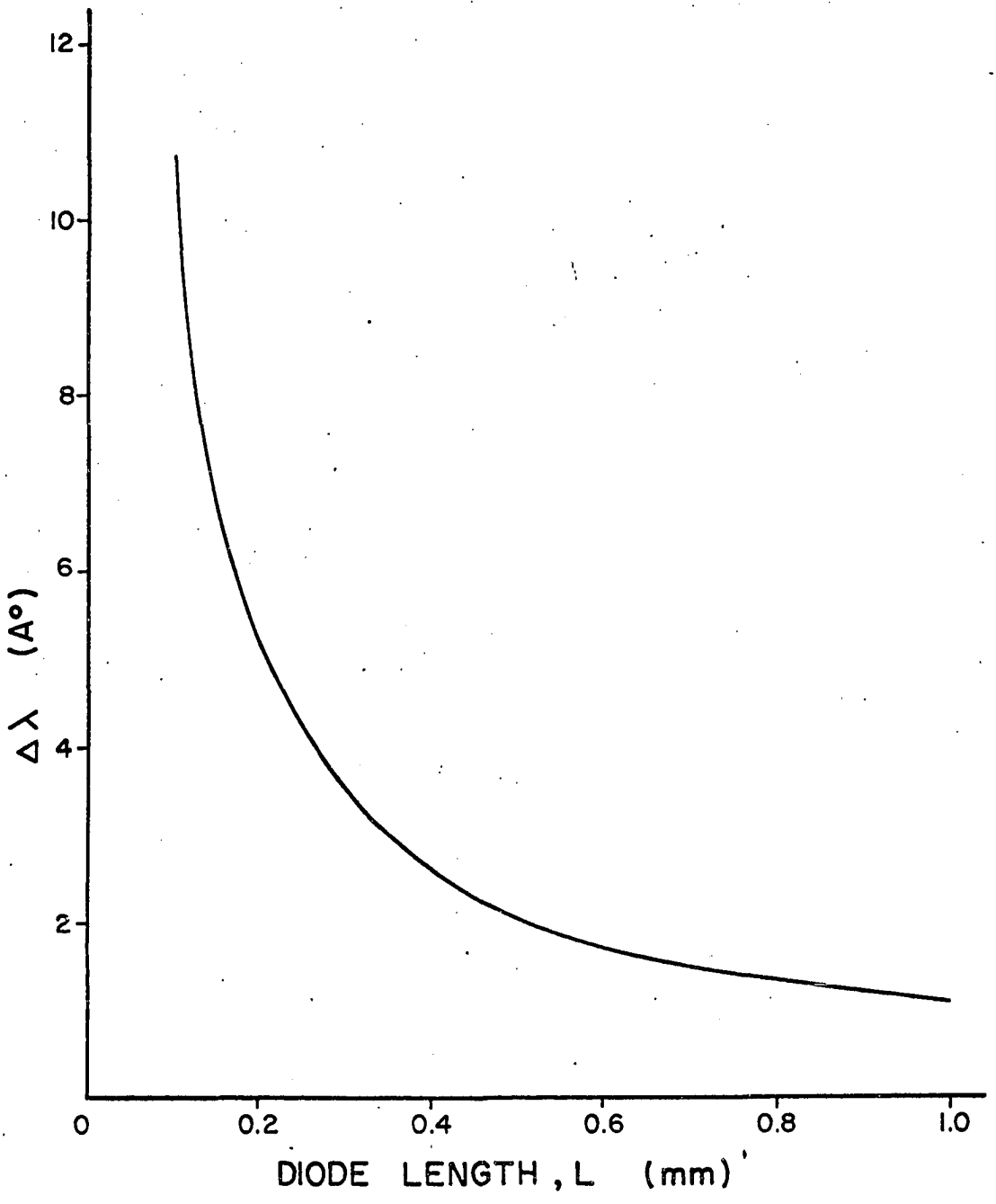

Figure 12. Theoretical relationship between the L and $\Delta\lambda$

value of L as 4200 A^{o}, then the crystal will sustain the 8400 A^{o} radiation. If instead the crystal is only 4100 A^{o} long, the first lasing wavelength will appear to be 8200 A^{o}. In this example the $\Delta\lambda$ is 200 A^{o}. As Figure 12 shows, this $\Delta\lambda$ will be much more reduced as the crystal dimensions are increased. However Figure 12 does not seem to agree with experiments at large values of L.

Equation 1 shows the equation for the reflection coefficients at the end of the crystal. Our discussions have been made with $\bar{n}$ equal to a real number. In practice $\bar{n}$ is complex. If $\bar{n}$ is some a + jb, then R is complex. If this complex $\bar{n}$ is substituted into Equation 1, one obtains

$$R = \frac{(a-1)^2 - b^2 + j2b(a-1)}{(a+1)^2 - b^2 + j2b(a+1)} \tag{14}$$

If $\bar{n}$ is close to being a purely real number, we can assume b is small and R can be approximated by

$$R \approx \frac{(a-1)^2 + j2b(a-1)}{(a+1)^2 + j2b(a+1)} \tag{15}$$

One can now assume that a is 3.3 which is the usually accepted value of $\bar{n}$. One can then obtain the expression

$$R = \frac{(2.3)^2 \angle \tan^{-1}\frac{2b}{2.3}}{(4.3)^2 \angle \tan^{-1}\frac{2b}{4.3}} \tag{16}$$

The result of Equation 16 is to show that if $\bar{n}$ is complex with a small imaginary part, the magnitude is about the same as if $\bar{n}$ is real. There is a net phase change due to the angle associated with the reflection coefficient. Thus Equation 8 is only a good approximation which does not allow for a complex index of refraction. It should be pointed out that in addition to this discussion, a complex $\bar{n}$ will result in an attenuation factor coming from the imaginary part of $\bar{n}$. By assuming a real $\bar{n}$, this problem is eliminated.

EXPERIMENTAL EMISSION

Experimental Procedure

The lasers which were fabricated with the techniques discussed earlier in this thesis were tested and operated in liquid nitrogen at a temperature of 77° K. Figure 13 shows the equipment arrangement which was used to measure and record the output emission. The dewar vessel is a double-walled pyrex flask with two flat pyrex windows through which the diode radiation is emitted. Round cylindrical dewar vessels (without flat windows) were tried but it was found that the diode radiation was badly dispersed with these vessels. The spectrophotometer consisted of a Jarrell Ash monochromometer with a linear variable-speed wavelength scanner and an RCA 7102 photomultiplier tube. This photomultiplier tube which has its peak response at 8400 A° was operated at a 1200 volt potential in accordance with the manufacturer's specifications. The monochromometer was capable of scan rates of 2, 5, 10, 20, 50, 125, 250, and 500 A° per minute. The 50 A° per minute scanning rate was used for the results shown in this thesis. The monochromometer utilized removable inlet and outlet slits. The data reported

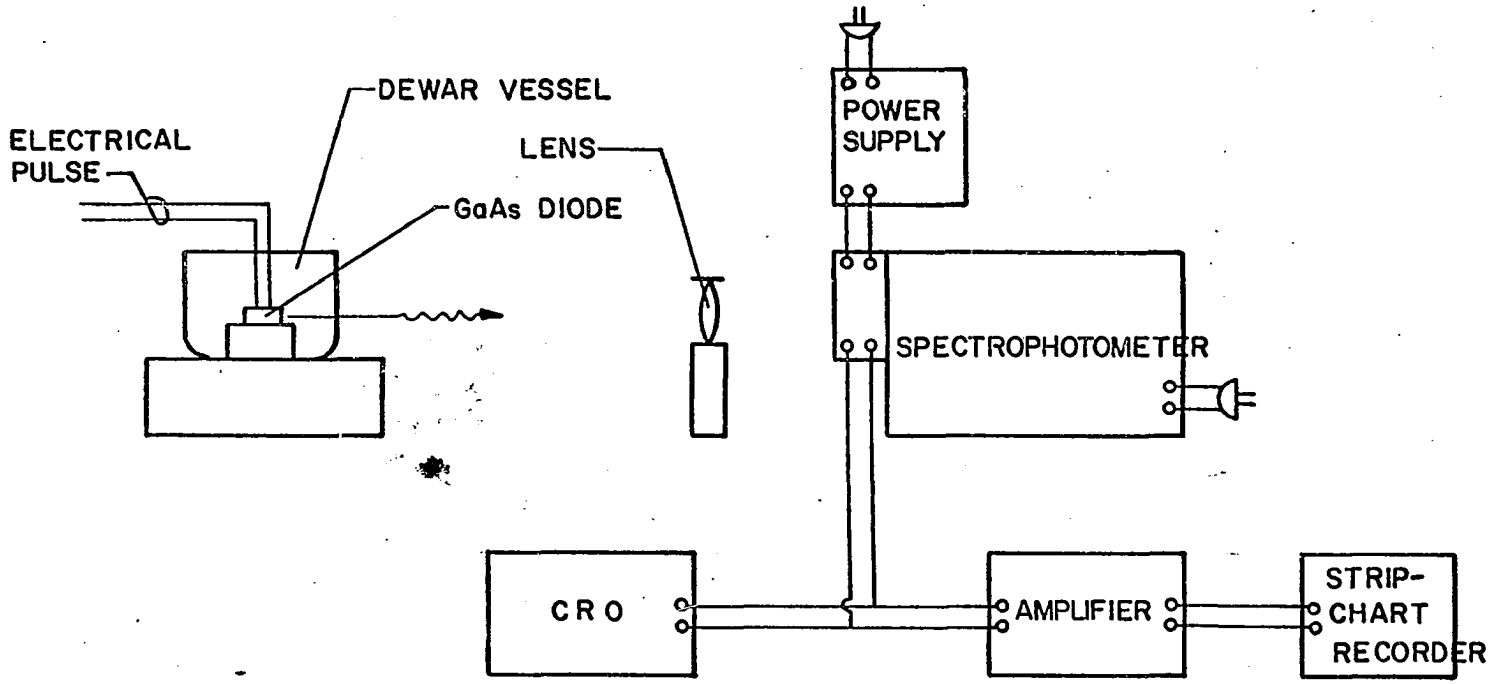

Figure 13. Sketch of equipment used to measure and record the laser output

in this thesis were taken while using 50 micron slits. With these slits in use, the monochromometer has a spectrum band-pass of 0.8 A^{o}.

Figure 13 shows two means of displaying the output radiation of the emitting diode. The cathode-ray oscilloscope (CRO) which was used was a Tektronix model 585. This CRO was used as a visual monitor of both the output radiation pulse and the input current pulse. The output of the photomultiplier was also recorded on a strip-chart recorder. This recorder utilized a Leeds and Northrup micromicroampere amplifier. The sensitivity range of the amplifier was set at 10^{-9} amperes for a full scale deflection.

In most instances, the lens in Figure 13 was a 25 centimeter focal length dual-convex quartz lens. In some of the experiments, however, a magnifying glass of undetermined focal length was used. Other lenses were occasionally placed in the beam but no major work was done with these lenses. Both the distance from the quartz converging lens to the slit of the spectrophotometer and the distance from the lens to the diode were 25 centimeters. When the magnifying glass was used as the converging lens, the slit-to-lens distance was about 8 inches while the diode-to-lens distance varied.

The emitting diode header was mounted as shown in Figure 14. The large brass base was soldered to the TO-5 transistor header. The large base served two purposes. It was a very good heat sink for the power dissipated in the emitting diode and the brass base formed a very stable platform on which to fasten the diode. The approximate dimensions of this base are indicated in Figure 14.

The emitting diode was pumped by an electrical current pulse. Although some diodes have been reported as being operated on direct current at a temperature of 77° K, such diodes are very special and such excitation is rare. Most GaAs diodes which are operated at liquid nitrogen temperatures must be pumped by an electrical current pulse. At 77° K, diodes of usable size (0.1 mm square to 1 mm square) may require current pulses having magnitudes from a few amperes to a few hundred amperes. To avoid excessive heating of the diode from Joule heating, the pulse width is usually maintained at about 1 to 10 microseconds while the pulse repetition rate can range from a few pulses per second to several thousand pulses per second.

Several different methods were tried in an attempt to generate the necessary pulses. These methods included

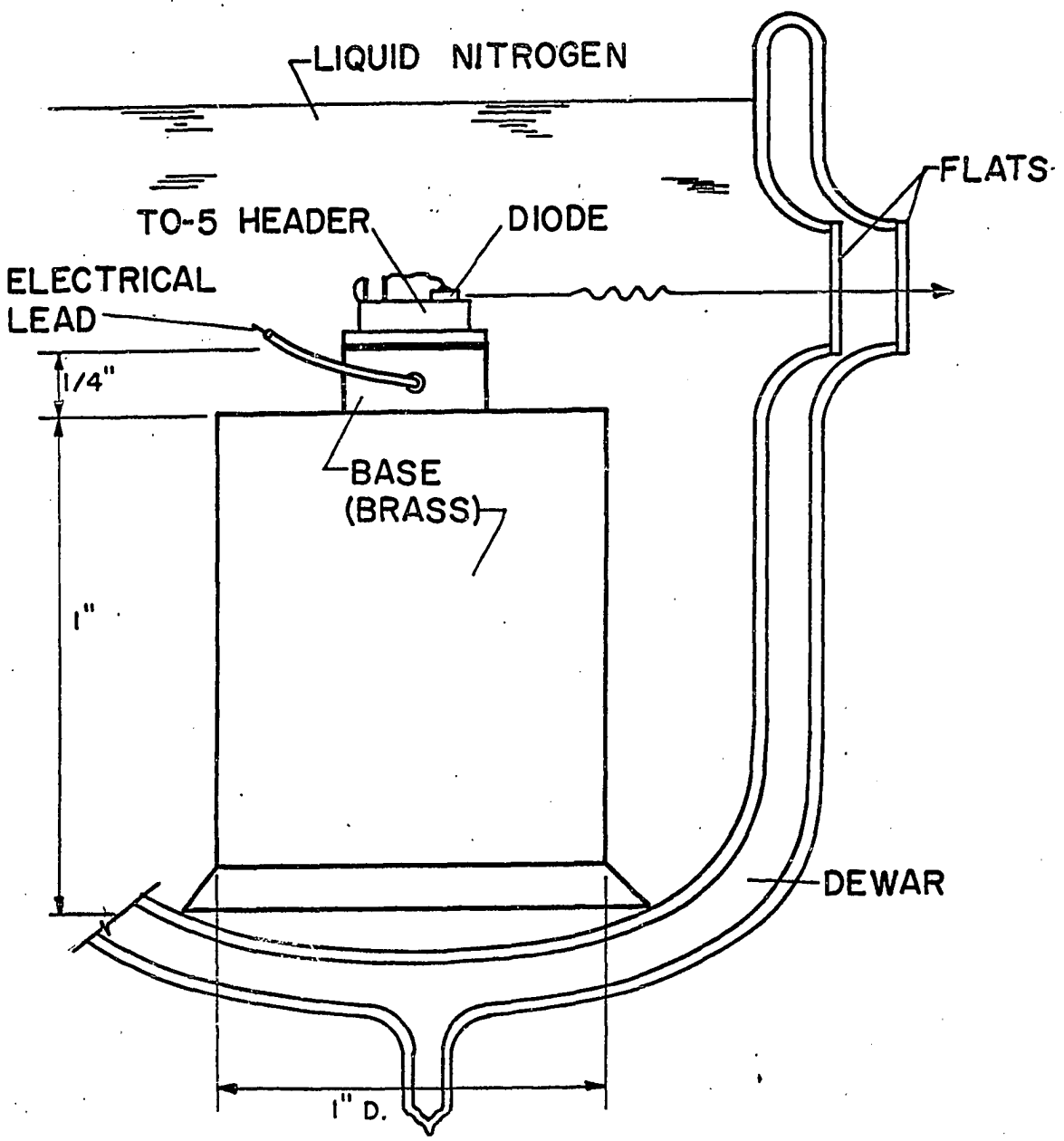

Figure 14. Dewar vessel and mounting base for diode laser

several different transistor amplifiers, pulse transformers, pulse generators, and some vacuum tube circuits. The outcome of all of these attempts was undesirable. A circuit designed after the circuit of Proebsting (17) was finally decided upon and is shown in Figure 15.

The power supply shown in Figure 15 has a range of 0 to 500 volts at 400 milliamperes. The pulse generator is a Hewlett Packard model 212A and is used as the gate trigger for the silicon controlled rectifier (SCR). The SCR is a TI 2N1604 and the three gate circuit diodes are TI 1N2071 solid state diodes. These diodes are necessary since the SCR must be protected against reverse currents in the gate circuit. It should be noted that the length of the coaxial cable shown in Figure 15 was about 6 feet. Cables up to 150 feet were tried. The pulse shape did not seem to be highly dependent on this cable length. Where possible, other interconnections including those shown in Figure 13 were made with coaxial cable to eliminate stray electrical pick-up.

Experimental Data

It was found that the unsilvered dewar flask continually emitted bubbles from its internal surfaces. These bubbles

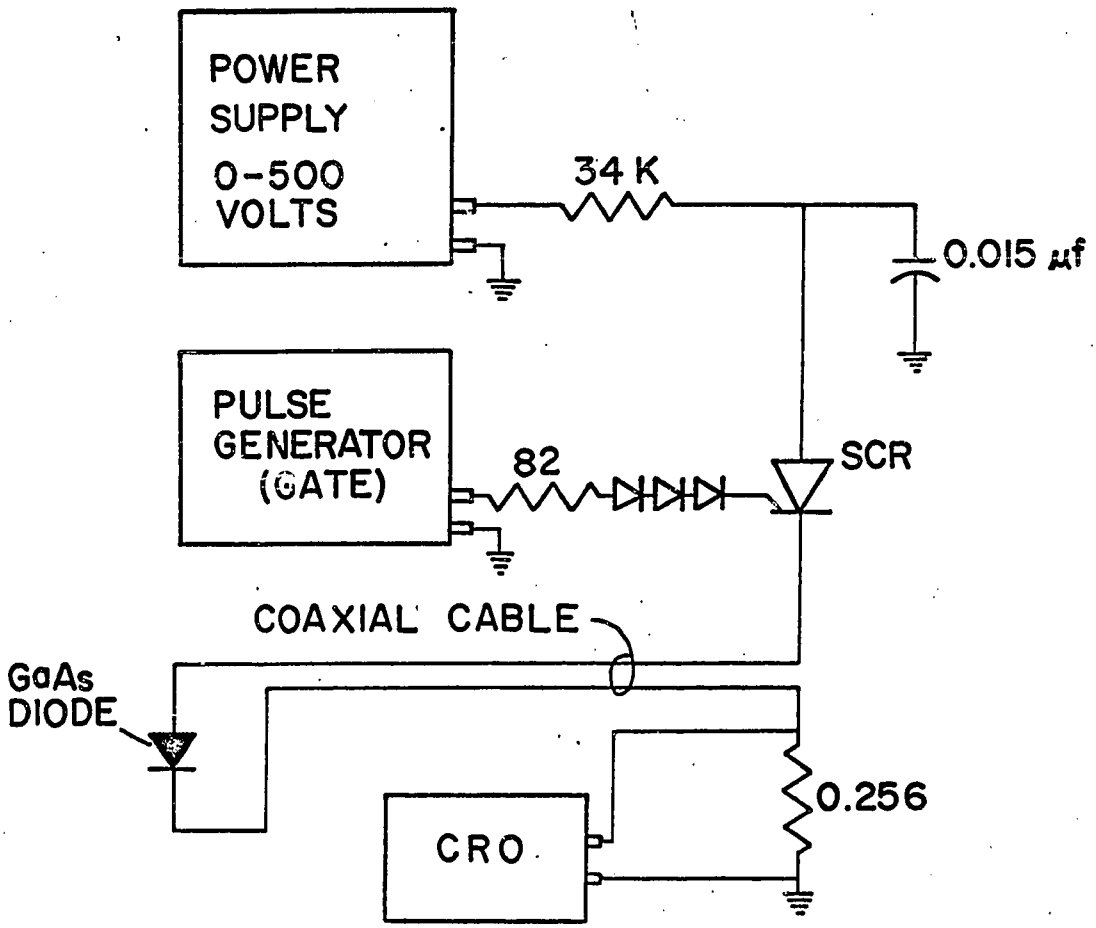

Figure 15. Schematic diagram of diode pulsing circuit

rose through the liquid nitrogen and passed through the path of the outgoing radiation. These bubbles in the radiation beam produced a scattering of the radiation and caused the output to be very erratic. Figure 16 shows the typical output of a lasing diode operated at 77^{o} K with the mounting shown in Figure 14. The erratic output was believed to have been caused by the scattering of the radiation by the bubbles. A one inch wide bubble shield was inserted parallel to the beam at the top of the heat sink. This shield forced the bubbles to the sides. This shield was fabricated from a piece of 1/16 inch thick aluminum sheet. Figure 17 shows a typical output after inserting the bubble shield. Upon comparing Figures 16 and 17 the assumptions concerning the causes of the erratic output were confirmed.

The data presented in this thesis were primarily concerned with the separate mode structure. With regards to previous discussions in this thesis, it could prove enlightening to check the output emission. Typical early attempts were similar to those shown in Figure 16. After the bubble shield was used, the results were much more stable and reproducible.

The main topic to be discussed is the mode shifts in the

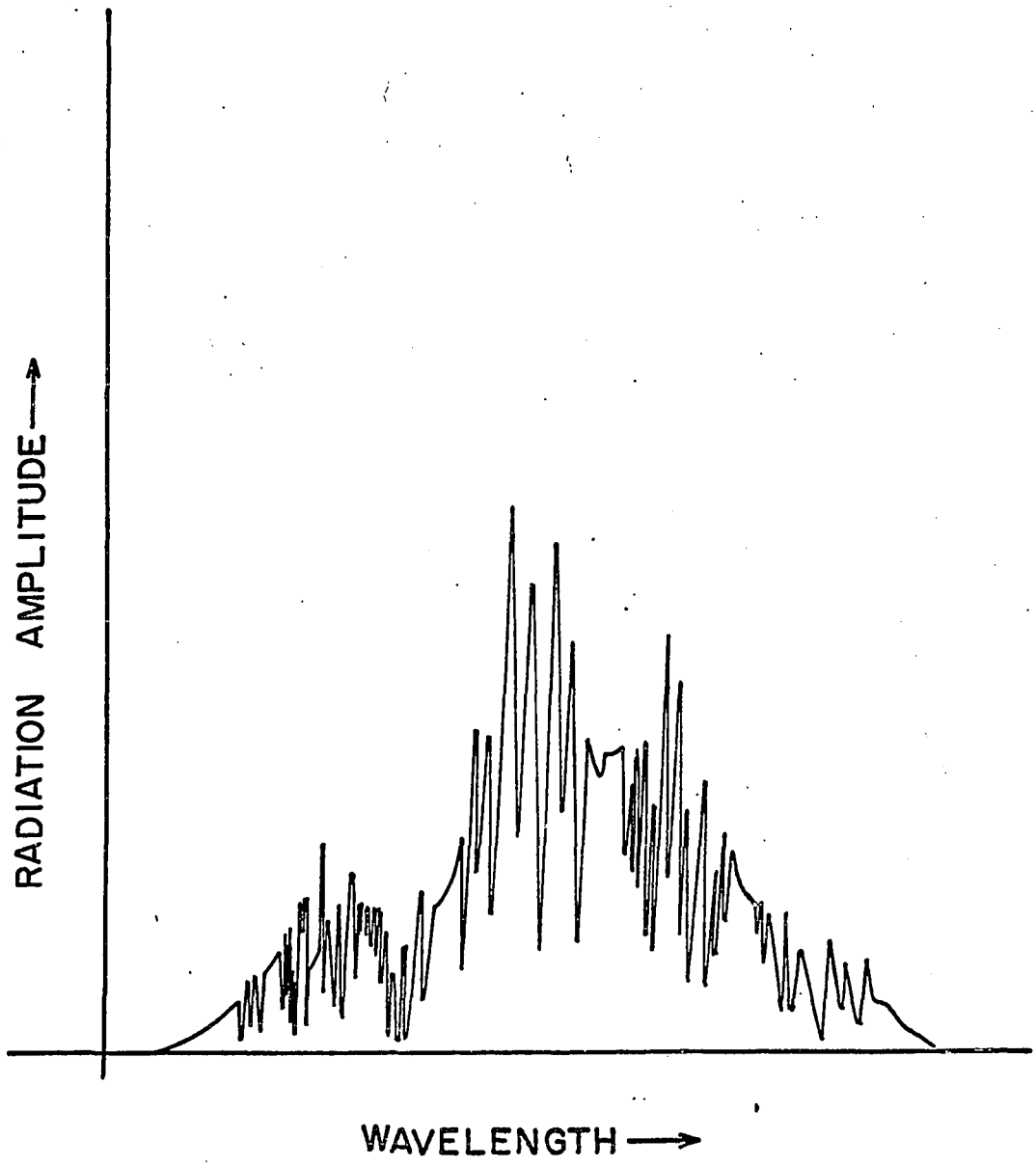

Figure 16. Typical laser output prior to installation of the bubble shield

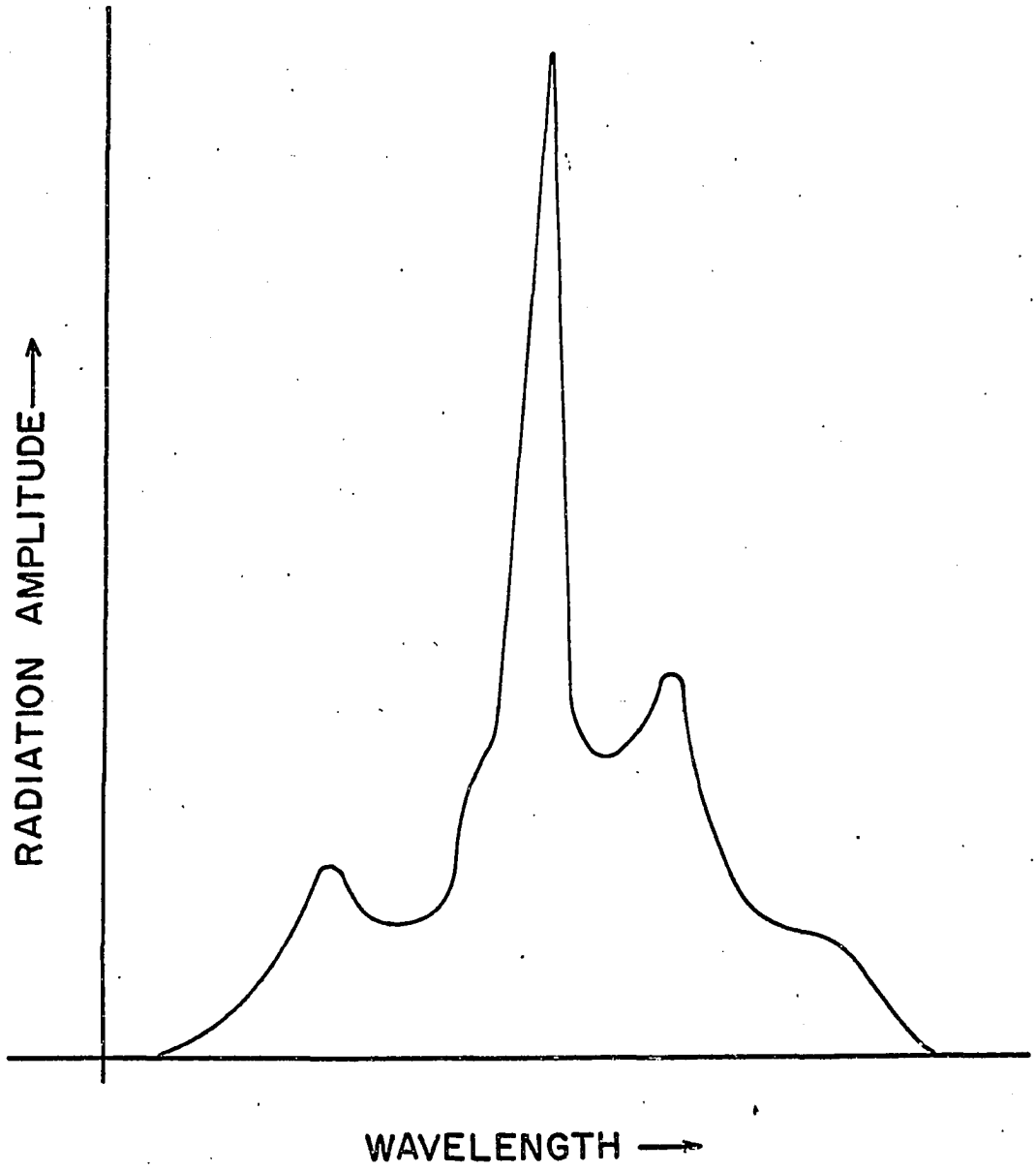

Figure 17. Typical laser output (same as Figure 16) after installation of bubble shield

emission output. Figure 18 shows the output of GaAs diode No. 100 just above the lasing threshold. This diode has dimensions of about 0.075 mm wide by 0.150 mm long and was prepared with cleaved ends and sawed sides. The threshold current is estimated to be about 2×10^4 amperes per square centimeter. It should be noted that in Figure 18 the peak output is at 8445.5 A^o. Separate modes do appear at other wavelengths but the dominant mode is at 8445.5. The current was increased slightly and the emission appeared as in Figure 19. Note that the 8445.5 A^o line was greatly enhanced and another sharp line began to appear at 8440 A^o. As the current was increased still more, the emission spectra appeared as shown in Figures 20 and 21. In Figure 21 the 8440 A^o and 8445.5 A^o lines are about equal in magnitude. Also noteworthy is the fact that the 8445.5 A^o line reached a maximum in Figure 20.

Figures 22 and 23 show the results of two more increases in current. In Figure 22 the 8440 A^o line is now clearly dominant while the 8445.5 A^o line is diminished but still clearly evident. Figure 23 shows the further enhancement of the 8440 A^o line while the 8445.5 A^o line is almost gone. Figure 24 is the result of still another increase in current.

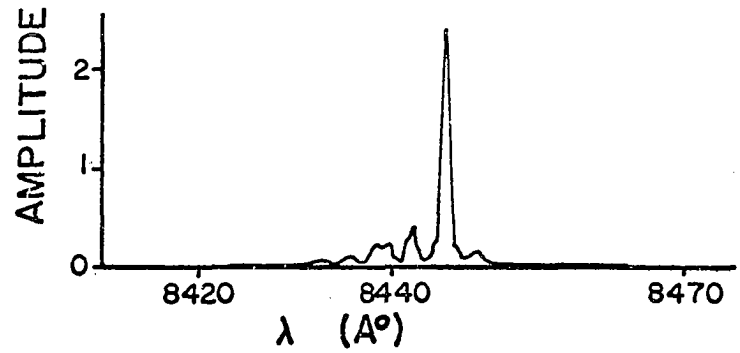

Figure 18. Output of diode number 100 with I equal to 2.34 amperes (just above threshold)

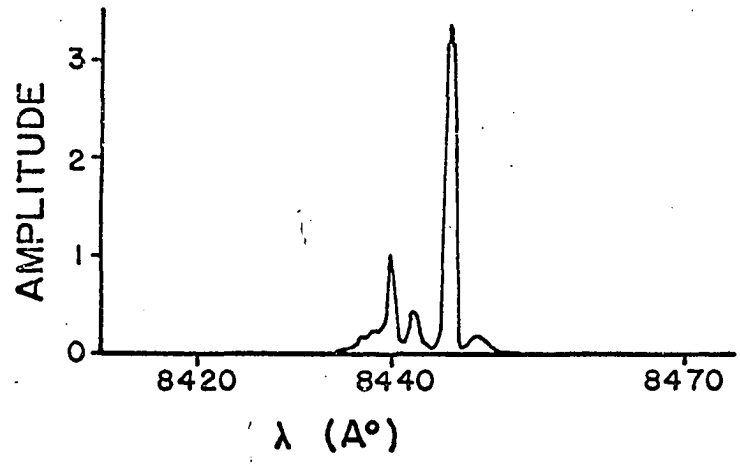

Figure 19. Output of diode number 100 with I equal to 2.42 amperes

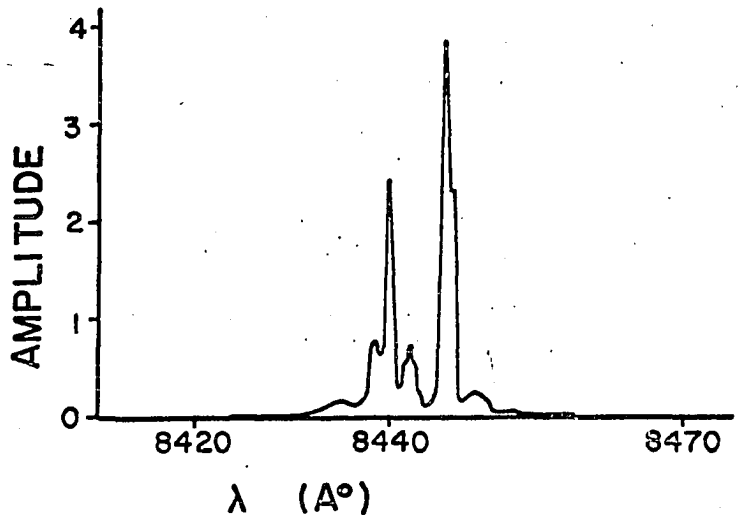

Figure 20. Output of diode number 100 with I equal to 2.50 amperes

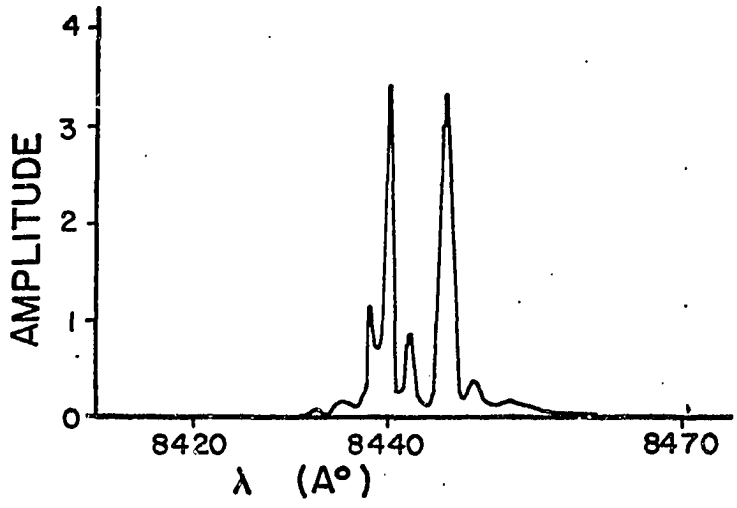

Figure 21. Output of diode number 100 with I equal to 2.58 amperes

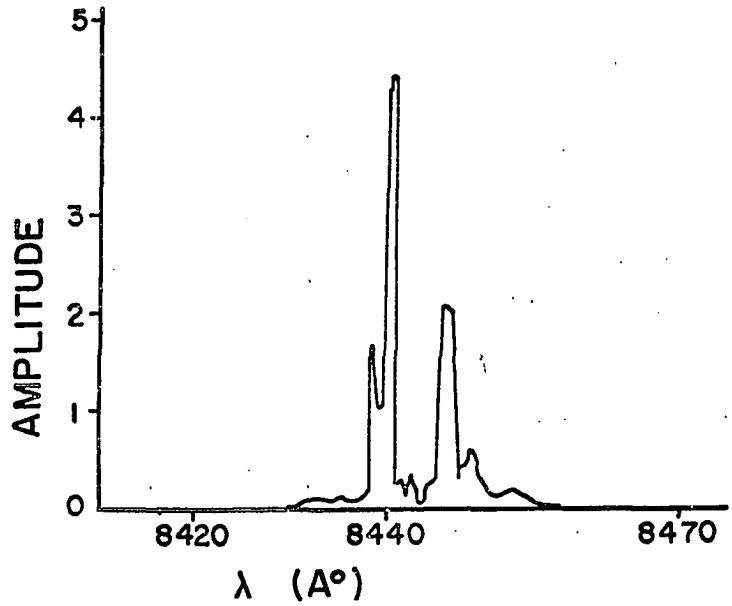

Figure 22. Output of diode number 100 with I equal to 2.66 amperes

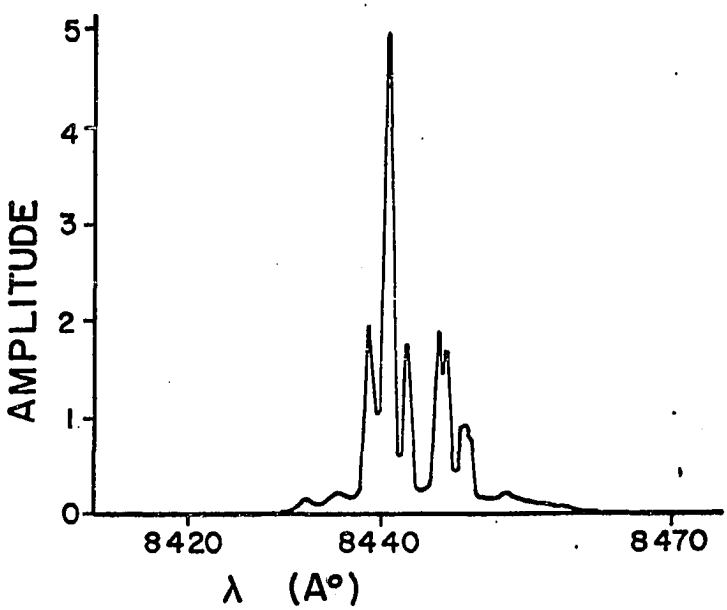

Figure 23. Output of diode number 100 with I equal to 2.74 amperes

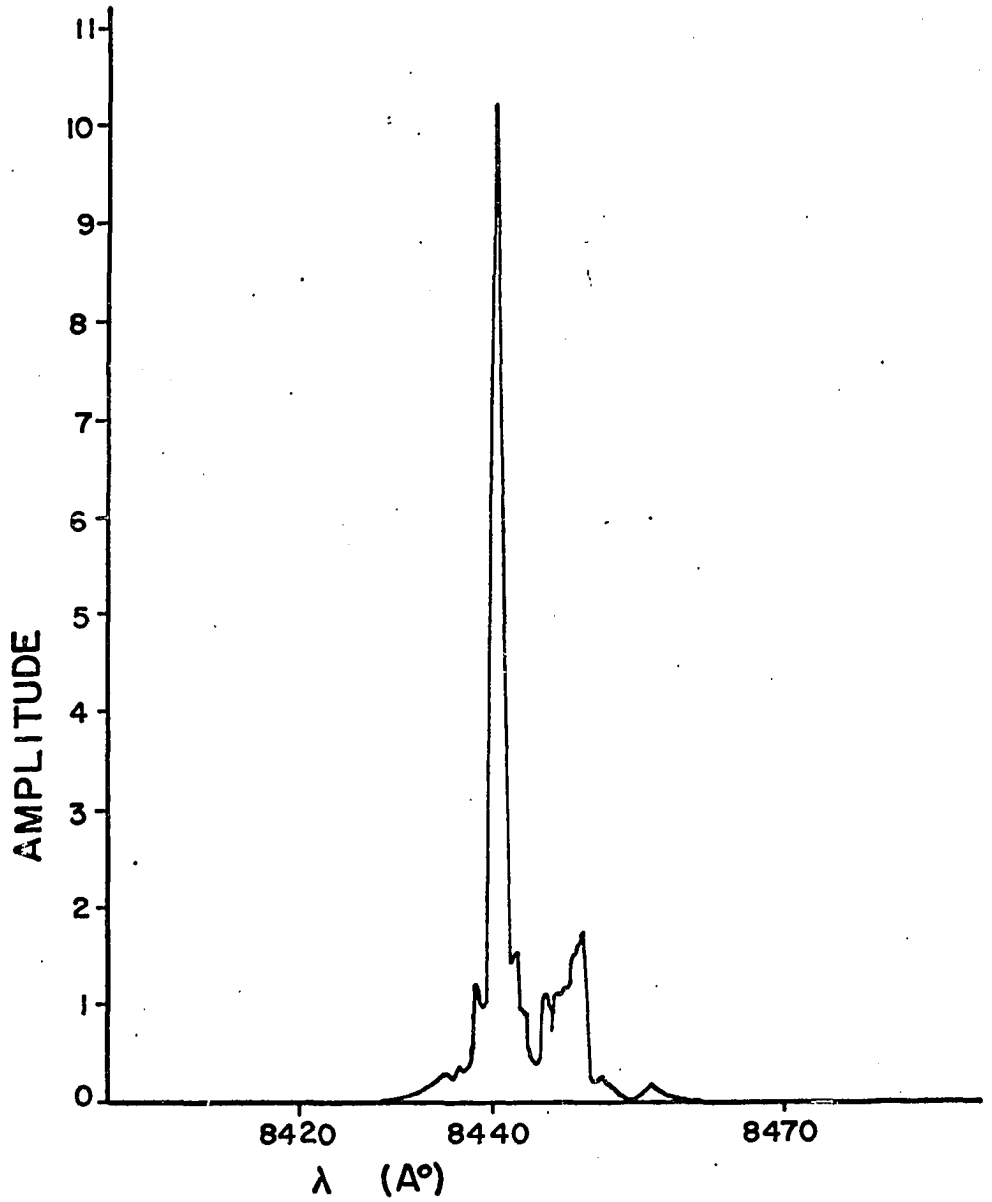

Figure 24. Output of diode number 100 with I equal to 3.04 amperes

This perhaps is the most vivid example of a good single mode laser output. There are clearly two distinct modes possible. However the 8440 A^{O} line now dominates completely. In Figure 24 if the spikes are disregarded, the radiation base is a gaussian emission distribution as reported by a number of authors. Figure 24 is the first of these figures to show strong background radiation levels. Figures 25 and 26 show the output for still higher current levels. Figure 25 still has the very dominant 8440 A^{O} line but the background radiation has increased. Figure 26 shows a sharp decrease in the 8440 A^{O} line and still larger background radiation levels. Further evidence of similar nature is shown in Figures 27 and 28. The Figures 18 through 28 constitute a family of curves showing the mode structure of the output emission with the current set at different levels. Similar behavior was noted in other diodes. The spectra in Figures 18 through 28 were obtained at a repetition pulse rate of 2000 pulses per second. Other repetition rates were tried with similar results. No upper limit of repetition rate was found because of limitations in the pulsing equipment. The threshold current levels were found to be constant over a frequency range from a few hundred cycles to

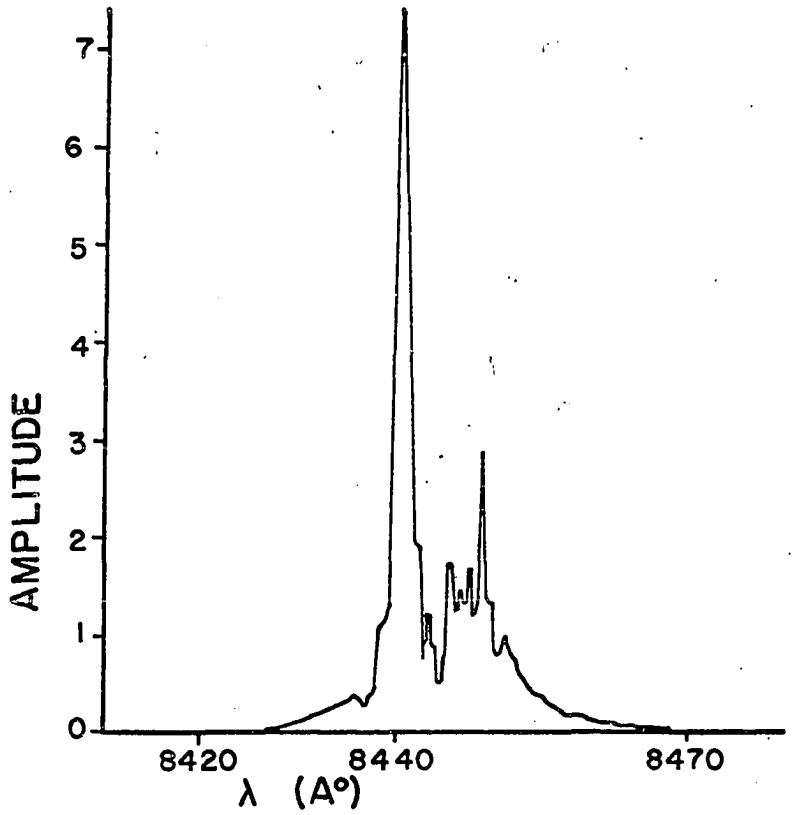

Figure 25. Output of diode number 100 with I equal to 3.12 amperes

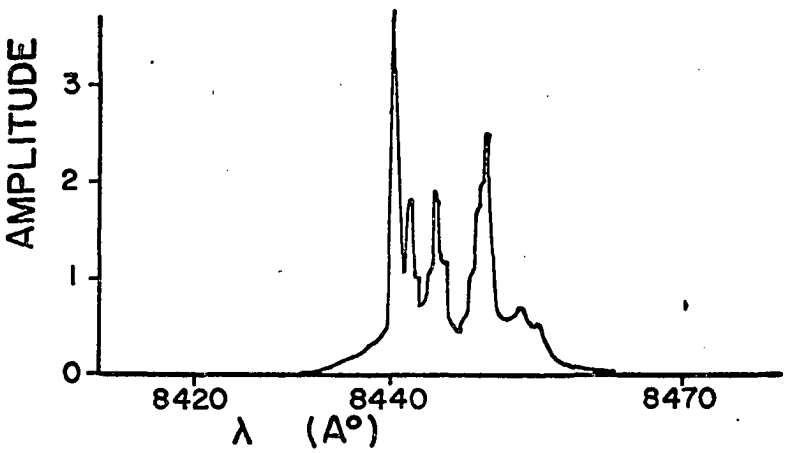

Figure 26. Output of diode number 100 with I equal to 3.52 amperes

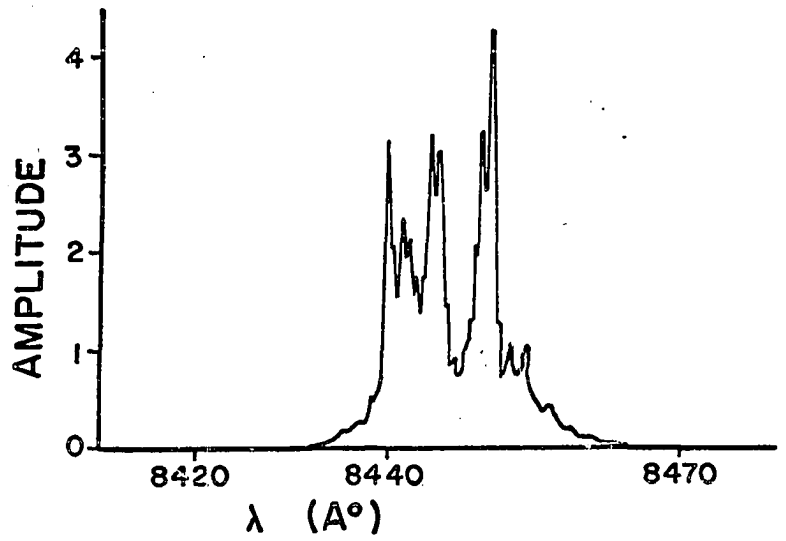

Figure 27. Output of diode number 100 with I equal to 4.68 amperes

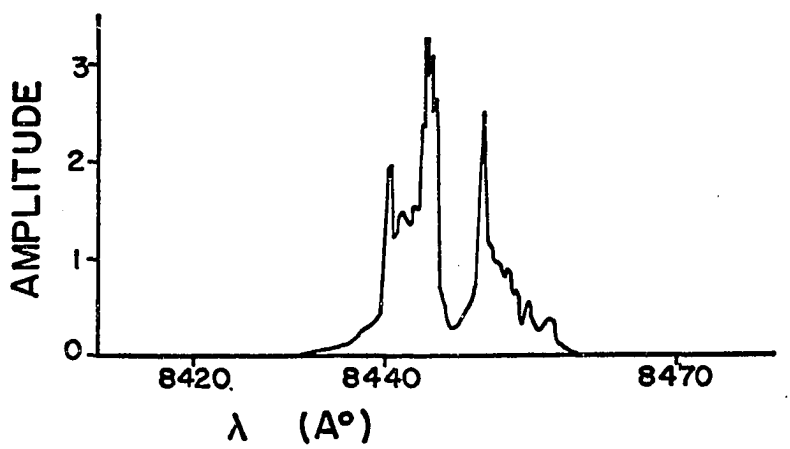

Figure 28. Output of diode number 100 with I equal to 5.65 amperes

a few kilocycles.

With data as shown in Figures 18 through 28, it is possible to plot the individual wavelength behavior as a function of current. This information is plotted in Figures 29 and 30. Figure 29 is from data taken from Figures 18 through 28. Figure 30 is taken from similar curves run at a repetition pulse rate of 1000 cycles. To compensate for the integration input of the strip chart recorder in Figure 13, the amplitudes in Figure 30 are twice the amplitudes recorded. This should make the amplitude scale of Figures 29 and 30 the same. The shape of these curves will be discussed in the next section of this thesis. Other data were taken but does not lend itself to graphical representation. These facts will also be mentioned in succeeding sections of this thesis.

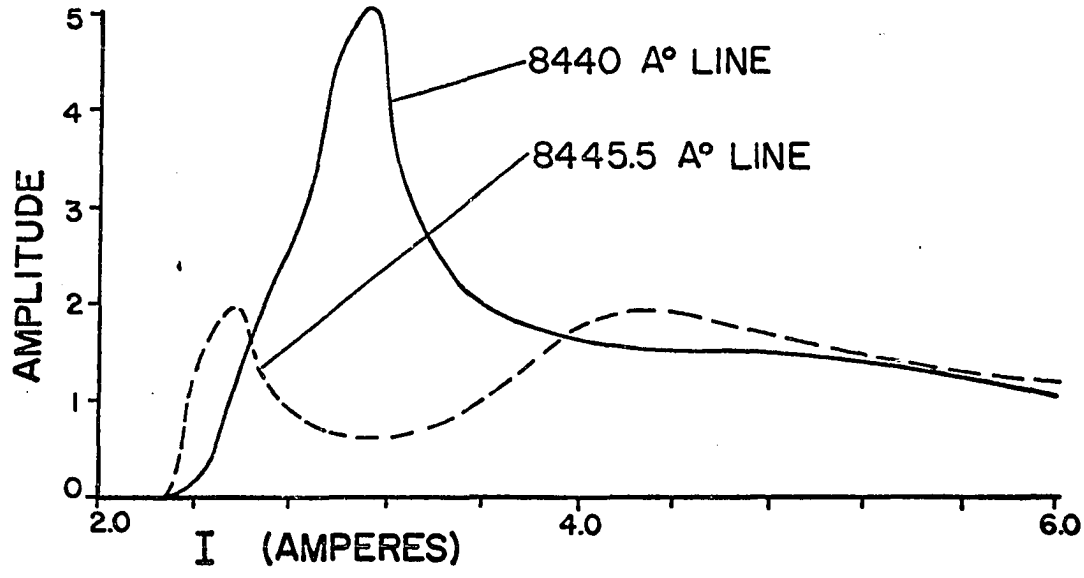

Figure 29. Output of diode number 100 pulsed at 2000 peaks per second

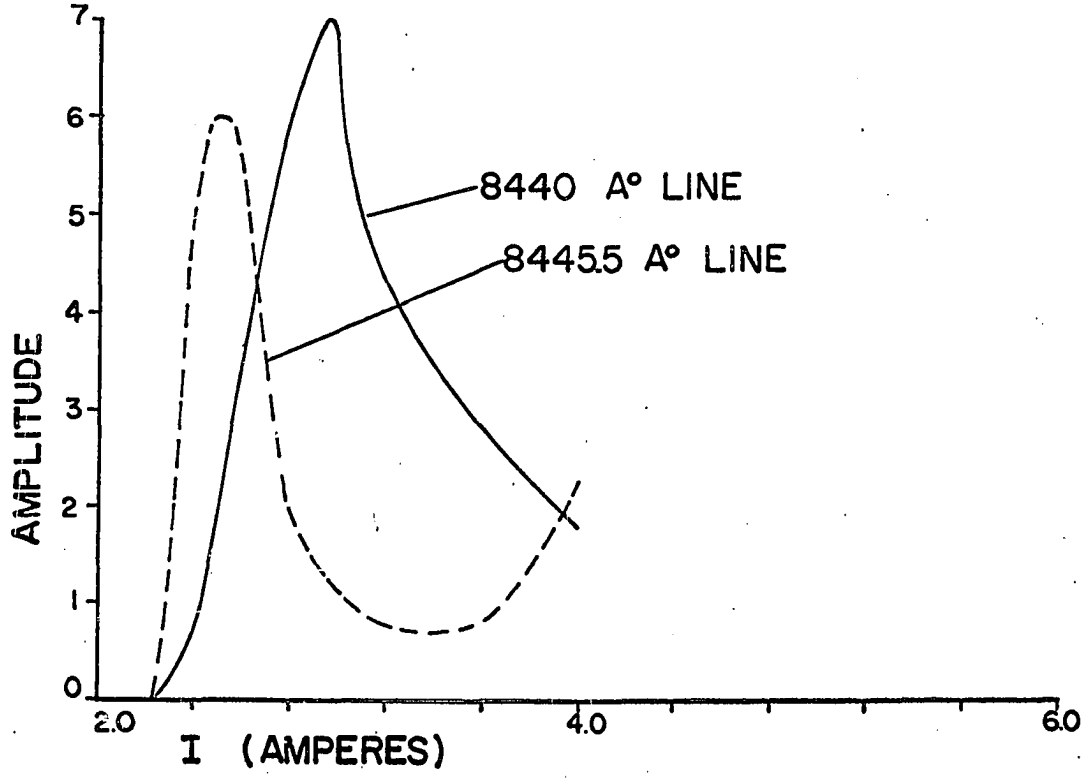

Figure 30. Output of diode number 100 pulsed at 1000 peaks per second

DISCUSSION

Nelson et al. (15) has described the radiation mechanism in GaAs in terms of a "band-filling model". He explained the data which he obtained in terms of an impurity band located just below the conduction band. Although lightly doped specimens of GaAs (concentrations less than 10^{18} impurities per cubic centimeter) could readily exhibit an impurity band located below the conduction band, in studies made on GaAs, Hilsum and Rose-Innes (7) state that the donor levels are actually merged into the conduction band at the concentration levels used in lasers. It seems that, instead of discrete impurity bands or donor levels, the net result would be to "smear-out" the lower edges of the conduction band. It might be stated that similar effects could occur at the valence band edges. Thus, at high donor concentrations, the conduction band's lower edge becomes very difficult to define.

As a first approximation, one might assume the conduction band's lower edge would be replaced by the lower edge of the donor band. It seems likely that electrons could move from the conduction band to the impurity band with the same freedom that electrons normally move in the conduction band. Thus we can arrive at a quasi-conduction band which exhibits

the behavior of the conduction band and has a band edge corresponding to the lower edge of the donor impurity band.

This merging of the conduction band and the donor impurity band is typical of a highly doped semiconductor acting metallic. The conduction band is well populated with donor electrons in the highly doped crystals usually used for lasers. The thermally induced carriers due to electron-hole pair production will be quite small relative to the impurity electrons.

It has been reported by several authors that the threshold current density for GaAs diode lasers decreases as the impurity concentrations increase. The population in this quasi-conduction band is largely dependent on the donor concentration. Thus, if the entire donor population contributes to this quasi-conduction band, the threshold current should decrease as the donor population is increased. Therefore this quasi-conduction band is in agreement with threshold current considerations.

With this idea of what the conduction band edges may look like, we can now attempt a theory to explain the behavior illustrated in Figures 18 through 28. The most striking part of the behavior is that the preferential lasing

mode shifts to a more energetic wavelength. When one looks through the papers published in recent years concerning GaAs lasing diodes, it becomes apparent that almost every diode exhibits several output wavelengths supposedly resulting from different modes of internal oscillation. However, only Howard (9) noted that there is an actual shift in this output wavelength. Howard was not actively investigating these shifts and therefore his comments were only qualitative. The important point to note from Howard's work is that the shift that he observed was from shorter to longer wavelengths of output radiation. Howard's work was done at 2^{o} K in liquid helium. The shifts in output wavelength which he reported were observed at currents somewhat higher than threshold (this is implied and not stated as a fact in Howard's publication). Such shifts to longer wavelengths can be partially explained by the geometric considerations discussed earlier in this thesis.

At 2^{o} K, the temperature effects due to pumping current are quite critical. Thus, as the diode temperature rises, the band gap energy decreases and when the band gap moves through an energy which is geometrically reinforced, a noticeable shift occurs. This shift will always be toward

longer wavelengths.

The emission reported in this thesis concerns a shift from a given radiation wavelength to a wavelength which is shorter. Notice that this is the exact opposite of the case reported by Howard (9). A second point to notice in Figures 18 through 28 is that the background radiation increases with current as does also the width of the emission spectra. The shift in the output emission can be due to heating effects, geometric effects as previously discussed, conduction band irregularities, or a combination of some or all of these.

The heating effects in GaAs diodes have been studied by many workers in the field. Although the results are generally empirical, widespread agreement among workers has been achieved. The heating of a diode should result in a somewhat steady transition to longer (less energetic) wavelengths. This transition has been explained in terms of the energy-gap variation as a function of temperature (-0.0005 eV/^{o}K). Therefore, any heating effects which are present should be of secondary importance in the shifting of modes since the observed shift is to shorter wavelengths. However, at high current levels the importance of heating becomes much

greater with respect to the output behavior.

Geometric effects were explained in an earlier section of this thesis. There is one effect which was not mentioned. If the current is increased a small amount, the temperature of the diode will rise. Because of thermal expansion, the dimensions of the crystal will change and the geometry of the crystal will change the output dominant mode. However, this change in the output at the dominant wavelength would again be a continuous change and would cover all wavelengths. Burns and Nathan (1) state that their information shows the change in dimensions cause negligible effects. This assumption was made in deriving Equation 9. Therefore, we must conclude that while the geometry does select those wavelengths which are enhanced, its effects also are secondary in explaining any jumps in the output wavelength. The geometry can account for the presence of different modes.

Another explanation of the two different dominant wavelengths might be that the two wavelengths represent exciton and band edge radiation. However, the energy separation between the wavelengths is much too small to be the exciton excitation energy and the exciton line has never been reported in lasers with high impurity concentrations.

If we try to formulate a model for the band structure of GaAs in the active laser region, it will look like that shown in Figure 31. At all current levels, the states below k_o are filled. Thus, all wavelengths between E_g and E_o are allowed with those near E_g preferred. The geometry could then choose those modes which are enhanced and these modes then become laser emission. If the current is increased to some I_1, the conduction band levels will be filled to an energy E_1 by electron carrier injection. Thus the number of possibilities of lasing wavelengths is increased. Hilsum and Rose-Innes (7) give adequate proof to show that these bands are parabolic. However there can be a large exponential tail as explained by Nelson et al. (15). Thus, we can see that as the rate of carrier injection into the depletion region becomes higher, we encounter more and more broadening of the number of occupied states in terms of wave number. The number of different stimulated wavelengths, however, does not increase in proportion to the current increase. This means that the dominant modes may be separated by fairly large current differences and that the number of available modes should increase slowly at high injection rates. This author has found no information to either prove or disprove

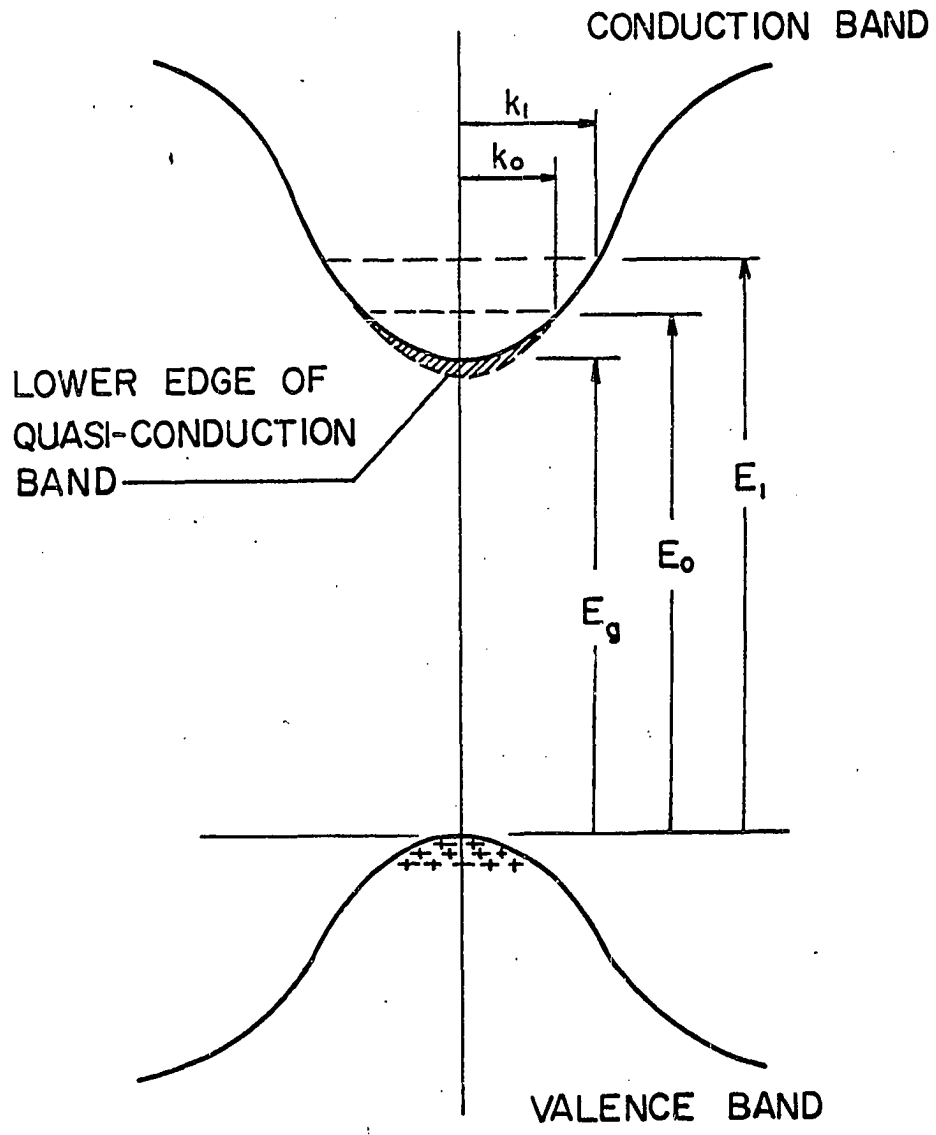

Figure 31. Proposed model of GaAs band structure

this point.

The next problem is to explain why the modes do jump from one wavelength to another. If there is a dominant mode at 8445.5 A^{o} as shown in Figure 18, then this mode should be present at all current levels unless for some reason, another mode should become more likely. This does not necessarily imply that the probability of the first mode is decreased. Several models could be theorized to explain the mode shifts. If the laser material is non-homogeneous, it is possible that different parts of the active region will emit different wavelengths and actually appear to behave like two different diodes. If there were small irregularities (adjacent maxima and minima) in the quasi-conduction band, different minima could contribute the different wavelengths. Another explanation might be based on the stimulation probabilities. If the transition probability for the 8440 A^{o} line is higher than the transition probability for the 8445.5 A^{o} line, then the 8445.5 A^{o} line could appear depressed at high current injection levels due to changes in the populations of both conduction and valence bands.

The actual mode shift may involve all of these causes in varying degrees. Much more work would be required to

definitely establish the cause of the mode shift. Figures 29 and 30 show that as the frequency of the drive pulse is increased, the current required for the peak output is also increased. While some of this shift can be attributed to thermal effects caused by diode heating, additional studies would be required to completely clarify this point.

In addition to the data already presented, some other interesting facts were noted. The diode's total emission reached a maximum at current levels about 3 or 4 times the threshold current. Above these currents, the total emission decreases and can be totally quenched at high current levels. These measurements were made by allowing the spectrophotometer band-pass to become large enough to encompass the emitted spectrum. This quenching effect is caused by the heating of the diode.

Although no definite data were taken regarding directionality, the usually directional qualities were noted.

Some experiments were carried out to exhibit the possibilities of short range communications using such diodes. It was found that very little intensity change occurred for distances between 2 feet and 13 feet. No distance beyond 13 feet were attempted since any practical system involving

longer distances would probably utilize some form of an optical lens system. The results of these studies were most favorable and short-range communications should be easily realized. One point should be mentioned at this time with respect to communications. The discussion earlier in this thesis mentioned scattering of the radiation by the bubbles in the liquid nitrogen. While it is recognized that communications will not usually employ a liquid nitrogen medium, the medium will contain water vapor, fog, dust, and smoke. For this reason, some consideration should be given to the problem of scattering when the laser beam passes through a non-homogeneous medium.

SUMMARY

The purpose of this thesis is two-fold. The first is to illustrate the methods of fabrication of GaAs lasing diodes. The second is to explain the expected and the actually obtained output spectra of these diodes.

The fabrication of a GaAs lasing diode can be divided into seven basic steps. These are: (1) crystal preparation, (2) junction diffusing, (3) polishing, (4) plating the contacts, (5) cleaving, (6) sawing, and (7) mounting the crystal. It is possible to achieve these steps with a minimum of equipment and with no controlled atmospheres. There are problems such as crystal orientation, etching the junctions and mounting the diodes. These steps are explained in detail in this thesis and all foreseeable problems are also explained. Methods for testing these diodes are given with examples of actual diode V-I characteristics shown. It is hoped that the result of the discussion of fabrication is to not only acquaint the reader with the techniques but to impress on him the idea that, with these techniques, it is rather simple (though lengthy) to produce solid state lasers. While this author recognizes the fact that GaAs lasers have been fabricated before, the fabrication sections

of this thesis are felt to represent a considerable contribution to research in this field. The important points to notice in other publications are that with few exceptions the techniques are seldom explained and that only the larger well equipped laboratories are producing these lasers. This thesis clearly demonstrates that, while some of the methods are time consuming, the techniques should not limit fabrication of these diodes to large well equipped laboratories. A method of fabrication is offered which should allow research in GaAs diodes to be easily carried on at the university level. This author feels that this in itself can represent a big step forward in laser research.

If diodes are successfully produced, one should be able to measure the output. This is perhaps the one most difficult task in laser production. After reading several papers written in the field of GaAs lasers, it was felt that a fair understanding of the expected output was obtained. This turned out to be about as far from reality as an "understanding" can ever be. In this thesis, actual output data are displayed.

It should be pointed out at this time that the data shown in Figures 18 through 28 are typical. These do not

represent the best examples of diode emission which were recorded. A point which some workers may ask concerns the quality of the data in light of the fabrication techniques. The data which were taken were in general at least as good as any thus far reported in the literature concerning GaAs lasing diodes. The output stimulated emission is a slow transition as the current is increased. It is not like a gas-laser in that one instant there is no output and the next instant there is a large output.

The solid state laser output is a continuous function of the input current. It was found that lasers were unknowingly being successfully fabricated for some time prior to being able to measure the output emission. To properly measure and display the output, the method shown in Figure 13 is recommended. The use of an oscilloscope to measure amplitudes of the radiation should not be attempted. Because of the pulse shape the oscilloscope was found to be inadequate. The strip chart recorder method is very satisfactory.

The actual measured data can be explained in terms of a quasi-conduction band which has the properties of the conduction band and an impurity band merged together.

Perhaps the major contribution in the thesis is the

observation and explanation of the wavelength shifts in the output. The observed shifts were to shorter wavelengths as opposed to earlier work by Howard (9) mentioning the opposite effect. An attempt was made to explain the results concerning the wavelength shift reported by Howard. Several possible theories were offered as possible explanations for the wavelength shift which was observed in the work reported in this thesis. It should be pointed out that the data reported in this thesis is based on two diodes which were constructed under very similar circumstances. Further studies could be made on different diodes to attempt to reproduce these results. Further research at this time is not planned because of problems in the extended availability of some of the required measurement equipment.

Additional information was reported on the method of measurement, and some aspects of short range communications. It was found that short range communications may be quite easily realized. This and other work was reported qualitatively only.

LITERATURE CITED

1. Burns, G. and Nathan, M. I. P-N junction lasers. Lithograph. IBM Watson Research Center Research Paper Number RC-1121. 1964.

2. Dekker, Adrianus J. Solid state physics. 1st ed. Englewood Cliffs, N.J. Prentice-Hall, Inc. 1957.

3. Dill, F. H., Jr. Gallium arsenide injection laser. Unpublished paper presented at International Solid State Circuits Conference, Philadelphia, Pennsylvania, 1963. Lithograph. Yorktown Heights, N.Y. Thomas J. Watson Research Center, IBM Corporation. 1962.

4. Dumke, W. P. Interband transitions and maser action. Physical Review 127: 1559-1563. 1962.

5. Fowler, Alan B. Quenching of gallium-arsenide injection lasers. Applied Physics Letters 3: 1-3. 1963.

6. Hall, R. N., Fenner, G. E., Kingsley, J. D., Soltys, T. J., and Carlson, R. O. Coherent light emission from GaAs junctions. Physical Review Letters 9: 366-368. 1962.

7. Hilsum, C. and Rose-Innes, A. C. Semiconducting III-V compounds. 1st ed. New York, N.Y. Pergamon Press. 1961.

8. Holonyak, Nick, Jr. and Bevacqua, S. F. Coherent (visible) light emission from $Ga(As_{1-x}P_x)$ junctions. Applied Physics Letters 1: 82-83. 1962.

9. Howard, W. E., Fang, F. E., Dill, F. H., Jr., and Nathan, M. I. CW operation of a GaAs injection laser. IBM Journal of Research and Development 7: 74-75. 1963.

10. Lasher, G. L. and Smith, W. V. Thermal limitations on the energy of a single injection laser light pulse. IBM Journal of Research and Development 8: 532-536. 1964.

11. Maiman, T. H. Stimulated optical radiation in ruby masers. Nature 187: 493-494. 1960.

12. Marinace, J. C. High power CW operation of GaAs infection lasers at 77 K. IBM Journal of Research and Development 8: 543-544. 1964.

13. Moss, T. A. Optical properties of semi-conductors. 1st ed. New York, N.Y. Academic Press, Inc. 1959.

14. Nathan, Marshall I., Dumke, William P., Burns, Gerald, Dill, Frederick H., Jr., and Lasher, Gordon. Stimulated emission of radiation from GaAs P-N junctions. Applied Physics Letters 1: 62-64. 1962.

15. Nelson, D. F., Gershenzon, M., Ashkin, A., D'Asaro, L. A., and Sarace, J. C. Band-filling model for GaAs injection luminescence. Applied Physics Letters 2: 182-184. 1963.

16. Phillips, Alvin B. Transistor engineering. 1st ed. New York, N.Y. McGraw-Hill Book Company, Inc. 1962.

17. Proebsting, Robert J. Gallium arsenide laser diode fabrication. Unpublished paper presented at Recent Advances in Solid State Technology Conference, Madison, Wisconsin, 1964. Mimeograph. Madison, Wisconsin. Electrical Engineering Department, University of Wisconsin. 1964.

18. Quist, T. M., Rediker, R. H., Keyes, R. J., Krag, W. E., Lax, B., McWhorter, A. L., and Zeiger, H. J. Semiconductor maser of GaAs. Applied Physics Letters 1: 91-92. 1962.

19. Sturge, M. D. Optical absorption of gallium arsenide between 0.6 and 2.75 eV. Physical Review 127: 768-773. 1962.

ACKNOWLEDGMENTS

The author wishes to thank Dr. A. A. Read for suggesting the subject of this thesis and for editing the thesis itself. Appreciation is also expressed to Mr. D. Anderson and Mr. T. Cowley for aid and loan of equipment to make this project possible. Without this equipment, the project could not have been accomplished. My thanks also to the IBM Corporation and Texas Instrument Corporation for their contribution of components and basic materials. The project was financed through the Solid-State Affiliates Research Program and the National Defense Fellowship Act. To those people mentioned above and to the people who offered aid and encouragement, the author expresses a very deep sense of gratitude.


65
464